Dynamical downscaling projections of late 21st century U.S. landfalling hurricane activity

Thomas R. Knutson[1], Joseph J. Sirutis[2], Morris A. Bender[3], Robert E. Tuleya[4], and Benjamin A. Schenkel[5,6]

[1]Geophysical Fluid Dynamics Laboratory/NOAA, Princeton, New Jersey

[2]Deceased

[3]Princeton University, Princeton, New Jersey

[4]Center for Coastal Physical Oceanography, Old Dominion University, Norfolk, Virginia

[5]Cooperative Institute for Severe and High-Impact Weather Research and Operations, University of Oklahoma, Norman, Oklahoma, USA

[6]National Severe Storms Laboratory/NOAA, Norman, Oklahoma, USA

Apr. 6, 2022 version

Climatic Change (accepted for publication, Mar. 15, 2022)

Corresponding author:
Thomas R. Knutson
Email: tom.knutson@noaa.gov

Abstract.

U.S. landfalling tropical cyclone (TC) activity was projected for late 21st century using a two-step dynamical downscaling framework. A regional atmospheric model, run for 27 seasons, generated tropical storm cases. Each storm case was re-simulated (up to 15 days) using the higher resolution GFDL hurricane model. Thirteen CMIP3 or CMIP5 climate change scenarios were explored. Robustness of projections was assessed using statistical significance tests and comparing changes across models. The proportion of TCs making U.S. landfall increased for the warming scenarios, due in part to an increased percentage of TC genesis near the U.S. coast and a change in climatological steering flows favoring more U.S. landfall events. The increased U.S. landfall proportion leads to an increase in U.S. landfalling category 4-5 hurricane frequency, averaging about +400% across the models; 10 of 13 models/ensembles project an increase (which is statistically significant in three of 13 models). We have only tentative confidence in this latter increase, which occurs despite a robust decrease in Atlantic basin category 1-5 hurricane frequency, no robust change in Atlantic basin Category 4-5 and U.S. landfalling Category 1-5 hurricane frequency, and no robust change in U.S. landfalling hurricane intensities. Rainfall rates, averaged within 100 km radius of the storms, are projected to increase by about 18% for U.S. landfalling TCs. Important caveats to the study include low correlation (skill) for interannual variability of modeled vs. observed U.S. TC landfall frequency and model bias of excessive TC genesis near and east of the U.S. east coast in present-day simulations.

1. Introduction

U.S. landfalling tropical cyclones (TCs, which include hurricanes and tropical storms) can cause major damage to coastal and inland infrastructure, and it is of great interest to better understand how landfallling TC activity may change under future anthropogenic climate change, with a particular focus on landfalling hurricanes. Relatively long records (since at least about 1900) are available for tropical storm, hurricane, and major U.S. hurricane landfalls (e.g., Vecchi and Knutson 2008, 2011; Klotzbach et al. 2020; Vecchi et al. 2021); these time series do not show any significant increases since 1900. This lack of a significant change contrasts with the case for global mean temperature, where a clear anthropogenic warming signal has been identified (IPCC AR5). This indicates that U.S. landfalling TC frequency in the above regions is not a strongly detectable anthropogenically forced metric over the past century.

A previous dynamical downscaling study of Atlantic TCs (Knutson et al. 2013, hereafter K13) explored the impact of global warming on several aspects of TCs, but focused mainly on the lifetime maximum intensity stage of TCs, by performing five-day high-resolution downscaling simulations of storms near their times of maximum intensity. Thus, K13 did not focus on the U.S. landfalling stages, which often were outside of the 5-day window simulated with their downscaling model. In the present study, we revisit K13, but focusing on U.S. landfalling storm activity. To accomplish this, we integrate the higher-resolution hurricane model forward for 15 days for each storm case study. Through this study, we aim to provide more societally relevant information about the potential damage impacts of the storms (in terms of intensity, frequency, rainfall at landfall) under various climate change scenarios.

Previous studies on possible future changes in U.S. landfalling TCs have reported model projections including: changes in vertical shear and potential intensity near the U.S. coastline (Ting et al. 2019); reduced probability of TC landfall over the southeastern U.S. and increased probability over the northeastern U.S. (Murakami and Wang 2010); decreased TC occurrence over the southeastern U.S. (Liu et al. 2018); increased TC occurrence over most of the eastern US for a downscaled CMIP5 model ensemble, but slight decreases for CMIP3 (Wright et al. 2015); reduced TC occurrence over the southern Gulf of Mexico and Caribbean (Colbert et al. 2013); increased average post-landfall TC rain rates over the eastern U.S. (Wright et al. 2015; Liu et al. 2018; Stansfield et al. 2020); and increased likelihood of faster-moving landfalling TCs in the Texas region (Hassanzadeh et al., 2020). The last study result is qualitatively in contrast to an observed finding for historical TC behavior: a significant reduction in propagation speed over the U.S. land regions since 1900 (Kossin 2019). This reduced propagation speed in observations over the 20th century was not reproduced in a historical forcing model simulation (Zhang et al. 2020) which covered most of the 20th century. However, Gori et al.(2022) project that over the eastern US, decreased TC propagation speeds and increased TC intensity will intensify TC rainfall events and, along with sea level rise, exacerbate US coastal flood risk by 2100. Levin and Murakami (2019) found that historical increases in anthropogenic climate forcing led (qualitatively) to increased frequency of U.S. major hurricane landfall in their model, although a significant increase in U.S. major hurricane frequency is not seen in observations since 1900 (Klotzbach et al. 2020) nor since the late 19th century (Vecchi et al. 2021).

Our study uses a two-step dynamical downscaling framework, together with tropical climate change projections from multiple CMIP3 and CMIP5 climate models-- the same models as used in K13. For the present-day simulations, the Zetac regional atmospheric model was run over 27 seasons in order to generate tropical storm genesis case studies. Each storm case was then re-simulated using the higher resolution GFDL Hurricane Model. In addition to the present-day runs, 13 CMIP3 or CMIP5 climate change scenarios were explored. As discussed in K13, the Zetac model does simulate hurricanes but only with intensities of up to about 50 m s^{-1} surface wind speed. For this reason, the second downscaling step using the higher-resolution GFDL hurricane model (with about 9 km spacing for the inner grid) was necessary.

2. Methodology and Present-day Simulation Evaluation

The methodology for our study is described in more detail in Supplemental Material. Our methodology mostly follows that in K13, Knutson et al. (2007), and Bender et al. (2010), and is described in detail in those studies.

2.1. Experimental Design for Present-day Hurricane Simulations

We performed control (present-day) simulations for 27 August-October seasons (1980-2006), and 27 "warm-climate" seasons based on modified versions of the 1980-2006 season boundary conditions. We first assess how well our two-step modeling system is able to simulate present-day Atlantic hurricane activity and its interannual variability using the time-evolving NCEP/NCAR Reanalysis I (Kalnay et al. 1996) to force the boundary and interior large-scale conditions. To assess the interannual variability vs. observations, for the present-day runs we simulated an expanded set of 37 years (i.e., 1980-2016). For reasons of computational expense we did not expand the climate changes runs to cover these additional years.

Tropical storm cases are identified in these three-month simulations using the automated TC search procedure described in Knutson et al. (2007), including a requirement for warm-core structure, surface wind speeds for the storm of at least 17.5 m s^{-1}, and total duration of tropical storm conditions of at least 48 hours (not necessarily consecutive).

Each individual tropical storm case from the Zetac regional model was then re-run as an individual 15-day case study using the GFDL Hurricane Model, which is a triply nested moveable mesh system with grid-spacing as fine as about 9 km. Ocean coupling in the model allows the storm to generate a "cold wake" in the interactive SST field as it passes over the model ocean. Each tropical storm case was initialized in the hurricane model beginning from the time it first reached tropical storm intensity in the Zetac model.

2.2. Evaluation of Present-Day Hurricane Simulations

Figure 1 compares the observed Aug.-Oct. (IBTrACS, version 4, revision 0, Knapp et al. 2009) and model simulated tropical storm genesis density and tropical cyclone (tropical storms and hurricanes) track density from the GFDL Hurricane Model runs. The observed tropical storm genesis points and tropical storm tracks from IBTrACS are based on the official Best Track data from the National Hurricane Center. Model tropical storm genesis occurrences are determined from the Zetac regional model runs (except for storms which failed to run in the hurricane model), and are based on the tropical storm identification scheme described in the Supplemental Material.

The comparison in Fig. 1 shows that the model framework generates more subtropical (higher latitude) genesis cases than observed, including along and near the U.S. East Coast. Similarly the TC days (track density) comparison (Fig. 1 c vs. d) shows more subtropical occurrence (25°-35°N) in the hurricane model than in observations, including near the U.S. East Coast. These model biases would be expected to affect US landfalling TC statistics. While the tropical storm genesis events in the Zetac regional model were confirmed to have warm core (tropical) characteristics, the evolving downscaled storms in the GFDL Hurricane Model were not monitored for such characteristics. Therefore it is possible that a small fraction of the simulated excess storm occurrence in the subtropical latitudes may be due to storms with extratropical or mixed tropical/extratropical characteristics. However, the GFDL Hurricane Model storms do not propagate poleward of about 38°N due to model boundary influences (Supplemental Material), which limits the likelihood of extratropical storm segments in our simulations.

A further test of the performance of our two-step downscaling model framework is a comparison of the year-to-year variability of August-October modeled storm counts with that from observations for tropical storms and different categories of hurricanes (Fig. 2). The model was provided only time-varying Atlantic basin SSTs, lateral

boundary conditions, and large-scale atmospheric circulation, applied via large-scale interior spectral nudging. If the model is still able to generate useful information about tropical storm, hurricane, and intense hurricane numbers and their year-to-year variation, this increases our confidence that the framework can translate information about atmospheric and SST variability and change (if reliable) into useful information about resulting hurricane activity.

The time series in the left column of Fig. 2 show that our downscaling framework is useful for simulating Atlantic basin-wide hurricane activity given specified large-scale atmospheric, oceanic, and SST conditions. Specifically, the system simulates the following correlations versus observations for 37 year series of Atlantic basin Aug-October storm counts: 1) all TCs (tropical storms and hurricanes): r = 0.77 (explained variance: 59%); 2) Category 1-5 hurricanes: r=0.68 (explained variance: 46%); 3) major (Category 3-5) hurricanes: r=0.56 (explained variance: 31%); 4) very intense (Category 4-5) hurricanes: r=0.31 (explained variance: 10%). Assuming independence among years, correlations above 0.33 are significant at the 0.05 level, so for all cases except Category 4-5 hurricanes the results indicate significant correlation. For the Category 4-5 hurricanes, which comprise a small number of cases compared to the other TC frequency metrics, the results are nearly statistically significant. Our regional modeling framework is not the first model to show such skill at hindcasting Atlantic basin-wide TC activity and its interannual variability (e.g., Zhao et al. 2009, Chen and Lin 2013, Murakami et al. 2016, and others). Ours is the highest resolution framework among these studies, which provides our study with some advantages in terms of simulating more realistic hurricane structure compared to coarser grid models.

Rising trends are evident in many of the basin-wide time series in Fig. 2 (a, c, e, g). The modeled trends are similar to observed trends, with the notable exception of basin-wide hurricane frequency (Fig. 2c) where the modeled trend is stronger than observed. The cause of the observed rising trends remains an unanswered research question. The time period (1980-2016) is relatively short for detection of a greenhouse gas warming influence, and both internal variability and changes in aerosol forcing are possible contributors to such TC-related trends (e.g., Dunstone et al. 2013, Yan et al. 2017, Murakami et al. 2020). Our simulations indicate only that changes in the large-scale environment (including SSTs) help to explain the observed rising trends but do not explain the causes of the environmental changes. Nonetheless, we expect that the observed Atlantic hurricane trends and tropical Atlantic SST changes since 1980 have multiple causes; several studies suggest the TC frequency increases are likely not primarily a response to increasing greenhouse gases alone (e.g., Murakami et al. 2020). Thus, the over-prediction of the observed trend in hurricane frequency (1980-2016) in our model does not invalidate the model's potential use for greenhouse gas-driven warming scenarios. Fig. 2 also shows that our model framework has a slight positive bias in basinwide TC frequency, hurricane frequency, and major hurricane frequency.

The model framework's performance is much less skillful for U.S. landfalling storm counts (right column in Fig. 2). None of the simulated time series of U.S. landfalling TC counts are significantly correlated with observed variations: 1) all TCs: r = 0.21 (explained variance: 4%); 2) Category 1-5 hurricanes: r=0.15 (explained variance: 2%); 3) major (Category 3-5) hurricanes: r=-0.07 (no explained variance).

The above results provide an important caveat to our study. While the two-step model framework is relatively skillful at reproducing the year-to-year variation of basin-wide tropical storm and hurricane counts, this skill does not carry through to U.S. landfalling counts. Thus, while the basin-wide results provide model-based evidence that the year-to-year variability in the basin-wide numbers is not random "weather noise" but rather is controlled to a large extent by large-scale environmental conditions, the U.S. landfalling count variations seem much more difficult to capture using our modeling framework. While we are not aware of many other modeling systems that can successfully simulate U.S. landfalling TC frequency, one exception is the HiFLOR model (Murakami et al. 2016), which has shown some skill in predicting seasonal U.S. landfalling TC frequency over the period 1980-2015, suggesting that there are large-scale controls on this metric that are not being well captured

in our two-step model framework. We hypothesize two mechanisms that may be important for our model's shortcoming with simulating U.S. landfalling TCs and their variation. First, the model has a bias toward too much TC genesis and TC occurrence near the U.S. East Coast, compared to the Gulf Coast region. This will degrade the model's ability to simulate interannual variations reliably. It is less likely that we have large issues with unrealistic steering flows, since we are nudging the large-scale winds and other variables toward realistic (NCEP Reanalysis) target in our modeling procedure. Our second proposed explanation for the model's shortcoming is that, U.S. landfalling activity is in general likely to be more difficult to hindcast skillfully using models compared to basinwide TC activity. This is because basinwide activity is strongly correlated with--and therefore appears to be largely controlled by--relative SSTs and vertical wind shear in the Main Development Region (MDR) of the tropical Atlantic. The MDR clearly has a relatively pronounced and correlated multidecadal variability in major hurricane frequency, SST, and wind shear (e.g., Yan et al. 2018). On the other hand, Kossin (2017) has shown that vertical shear near the U.S. coast varies in opposition to that in the MDR such that when conditions are favorable in the MDR for TC development, they tend to be less favorable for TCs near the U.S. coast (i.e., high vertical wind shear). This characteristic of the Atlantic basin climate suggests that the task of simulating the interannual variability of U.S. landfalling TCs will be inherently more complex than for basinwide variability, owing to the competing influence of conditions in the MDR vs. near the U.S. coast, which corrupts an otherwise simpler multidecadal signal.

Despite the limitations of our framework at simulating interannual variability of U.S. landfalling TCs, we have still chosen to use our model explore future U.S. landfalling behavior under global warming in this study. We justify this decision by recognizing the importance of the issue for stakeholders and the need to take advantage of our model's high-resolution capability for simulating intense hurricanes and storm structure.

2.3. Specification of Climate Change Downscaling Simulations

Following on the above present-day simulations, here we analyze similar sets of experiments under climate change conditions. We focus here on 27 seasons (1980-2006) for computational efficiency.

We first created a series of climate change "delta" fields for SST, surface pressure, air temperature, relative humidity, and winds, which we added to the NCEP/NCAR Reanalysis, to create a series of warm-climate perturbation experiments that use realistic conditions (i.e., the reanalysis) as the baseline case. The warm-climate conditions were for the CMIP3 models (ensemble mean or 10 individual models) based on years 2081-2100 minus 2001-2020 of the Special Report on Emission Scenarios A1B (SRES A1B) scenario. We constructed two 18-model ensemble-mean CMIP5 model warm-climate scenarios using the 2016-2035 (early 21st century) or 2081-2100 (late 21st century) period of the CMIP5 RCP4.5 scenario versus a baseline period of 1986-2005. The global temperature difference between present-day and late 21st century warm-climate condition was 1.69^{o}C for the CMIP3 and 1.70^{o}C for the CMIP5 ensemble means.

3. Results of Climate Change Downscaling Experiments

In this section, we examine the results of our climate change downscaling experiments. In the discussion below, we refer to the 13 sets of experiments as 13 different "models", even though these can be based on an individual model, or on ensemble mean climate change from a set of CMIP3 or CMIP5 models.

A number of TC metrics were examined for our 13 different sets of experiments (see Table 1 of Supplemental Material for a complete set). To focus on results from our experiments where most models agree on the sign of the projected changes, we present the results for selected TC metrics in a summary form (Figs. 3 and 4) showing both the level of agreement across the models for projected changes for a given metrics, along with statistical significance test indicators for the individual model results. Using this approach, Figs. 3 and 4 examine two distinct but important sources of uncertainty in projections: modeling uncertainty as indicated by the

agreement in sign of the projected change for the 13 different models, and internal variability uncertainty, as assessed by the statistical significance tests. Both U.S. landfalling TC frequencies (or surface wind intensities and precipitation rates at the time of landfall) and the basin-wide results are summarized in Figs. 3 and 4. Basin-wide results are based on either conditions at the time of maximum storm wind speed intensity for the storm, or on the entire lifecycle of each TC in each year for the case of accumulated activity metrics like duration, propagation speed, or the PDI (Power Dissipation Index). The mechanisms behind the changes summarized in the Figs. 3 and 4 will be explored further in Section 4 (Discussion).

3.1. TC Frequency Projections

Figure 3 (a) indicates that a robust projection is a decrease in basin-wide hurricane frequency (Category 1-5). A decrease is simulated in 12 of 13 models (statistically significant in 9 of 13 models), with an average decrease across all models of -34%. Detailed data (in Supplemental Material) indicates this decrease is particularly robust for basin-wide frequency for: category 1 hurricanes (-42%), category 2 hurricanes (-45%), category 3 hurricanes (-43%), all tropical storms and hurricanes combined (-28%), all hurricanes combined (category 1-5; -34%), and major hurricanes (category 3-5; -25%). In contrast, the most intense (Category 4-5) hurricanes show little consistent change in basin-wide frequency with warming (panel b), with seven (six) of 13 models projecting a positive (negative) change.

This contrasting behavior of Atlantic basin hurricanes vs. intense hurricane frequency has been discussed previously (K13) and is related to the increase in the average intensity of the TCs in the model, as will be discussed further below. Comparisons with other studies, for example, Knutson et al. (2020) show that the majority of published projections of Atlantic overall TC frequency (tropical storms plus hurricanes) indicate a decrease in frequency with climate warming, but an increase in the frequency of Category 4-5 TCs. However, there is a wide variation in these projections across models for both all TC frequency and Category 4-5 TC frequency, with some disagreeing on even the sign of the change. However, a relative increase of Category 4-5 TC frequency compared to all-TC frequency is a consistent feature of the multi-model TC assessment in Knutson et al. (2020). A recent attempt at better understanding the controls on TC frequency change in models has focused on the role of seed disturbances (Hsieh et al. 2020).

U.S. landfalling TCs (Fig. 3 c,d) show a contrasting behavior to the highly significant and robust decreases seen for basin-wide TC frequency. In particular, there is no robust increase or decrease for U.S. landfalling Category 1-5 hurricane frequency (panel c). On the other hand, for U.S. landfalling category 4-5 storms (panel d), the average change across models is +390%, with at least nominal increases for 10 of 13 models, and statistically significant increases for three of the 13 models. No change was found for three models. The projected increase in U.S. landfalling Category 4-5 hurricane frequency is noteworthy from a climate impacts perspective because these storms have historically caused almost 50% of normalized TC damage in the U.S., despite representing only 6% of historical TC occurrences (Pielke et al. 2008). As a sensitivity test, we have assessed U.S. landfalling category 4-5 frequency based on surface pressure, rather the surface wind speed criteria (not shown)and found similar though slightly less statistically robust results

To visually illustrate this relatively important finding in Fig. 3, Fig. 5 shows the tracks and intensities of the simulated U.S. landfalling hurricanes that are category 4 or 5 at landfall. A clear tendency for an increase in these very intense landfalling cases is seen across downscaled storms from most of the models, including the CMIP3 and CMIP5 late 21st century ensembles.

The differing response of basin-wide vs. U.S. landfalling TC frequency to climate warming indicates that the proportion of TCs making U.S. landfall increases in the projections-- according to most models. Figure 3 (e) shows, for example, that for all hurricanes (Category 1-5), the proportion making U.S. landfall is projected to increase by all 13 models, with an average increase of 64% above the control proportion value of 0.12. Similarly, for Category 4-5 hurricanes, the proportion of such storms making U.S. at Category 4-5 intensity increases by

+350% over the control run fraction of 0.024, with an increase projected for 12 of 13 models. Increases in U.S. landfalling proportion for other classes of TCs are shown in the Supplemental Material.

3.2. TC Rain Rate Projections

Climate change projections for several other TC metrics are summarized in Fig. 4. Increasing TC precipitation rate with climate warming has been identified as among the most robust projections for TCs across different modeling studies (Knutson et al. 2020; Liu et al. 2018, 2019; Stansfield et al. 2020; Gori et al. 2022). Fig. 4 (a) shows a robust increase for TC rainfall rates at (or just prior to) U.S. landfall (+18% on average across the models), based on rain rates averaged within 100 km of the storm center. Eleven of 13 models show increases in this metric, while three of 13 show statistically significant increases. For basin-wide TCs, a statistically more robust increase in TC rain rates is projected (Table 1, in Supplemental Material) with an average change of +19%, positive in 12 of 13 models, and statistically significant increases in seven of 13 models. The more significant projected climate change signal in basin-wide TC rain rates (for roughly the same sized climate change signal) is probably due to the larger sample size available vs. the U.S. landfalling subset of storms.

3.3. TC Intensity Projections

Maximum lifetime hurricane intensity (based on modeled near-surface (10 m) wind speeds) is a metric which relatively higher resolution models have consistently projected to increase with climate warming (Knutson et al. 2020). Figure 4b shows that the hurricane (Category 1-5) intensity increases in our experiments are robust for the Atlantic basin as a whole, with all but one of 13 models showing an increase, significant for six of 13 models. For U.S. landfalling hurricanes (Fig. 4d), the projected intensity changes are more mixed, with seven of 13 models showing an increase and only one being statistically significant. The U.S. landfalling hurricane intensities are based on intensities in the model at or just prior to the time of landfall.

The one outlier model for basin-wide hurricane intensity change is the CMIP3 HadGEM1 model, for which we simulate a significant decrease. As discussed in K13, this particular model exhibits a much more enhanced warming of the upper tropical troposphere (compared to the surface warming) than other CMIP3 models. Such amplified upper tropospheric warming has been shown to a detrimental factor for modeled TC intensification (Tuleya et al. 2016).

The average TC intensity change across the 13 models is about +5%. This result is relatively consistent with other high-resolution modeling studies (Knutson et al. 2020). Interestingly, the increase is absent if one includes weaker (tropical storm-strength TCs) in the sample, but we consider the hurricane intensity result as the more relevant one for potential climate impacts. In summary, despite the increase in basin-wide hurricane intensity, the average intensity of landfalling hurricanes shows little significant change, nominally averaging about +2%.

3.4. TC Translation Speed, Duration, and Power Dissipation Index Projections

Figure 4 (c) indicates that the basin-wide TC translation speed tends to increase in the models, with 10 models projecting an increase (only two are significant) and three models projecting a decrease. As will be illustrated later in this report, the two models with significant translation speed increases both have substantial increases in easterly steering flow in the central tropical Atlantic, which leads to faster westward propagation across that region. Average TC duration (Fig. 4 e) shows a clear tendency to decrease by about 13% on average (decreasing in 12 of 13 models, with 8 of 13 models projecting a significant decrease). The slight increase of translation speed may be one factor contributing to a decrease in duration, as the lifecycle of the storm over a given track would be shortened by the faster propagation speed. Furthermore, the greater fraction of TCs making U.S. landfall in the warm climate runs means that more storms have truncated lifetimes as they dissipate after U.S. landfall as opposed to recurving out to sea without encountering land. Also storms forming closer to the coast will tend to have shorter lifetimes before they dissipate over land compared to storms forming further away

from the coast. However, we have not quantitatively diagnosed the reasons for the decreased duration under climate change in detail. Duration of storms in the model (both control and warm climate cases) can also be artificially limited by the 15-day limit of the simulations and by the effective northern boundary near 38oN (Supplemental Material). Finally, Fig. 4 (f) shows that the Power Dissipation Index (PDI, see Supplemental Material) has a robust projected decrease, with a decrease simulated in 11 of 13 models (averaging -28%), and with five models projecting a statistically significant decrease.

4. Discussion

In this section, we discuss mechanisms behind several key model projections, and provide some assessments of our confidence in the projections.

4.1 Increase in Proportion of TCs Making U.S. landfall

A potentially important finding in our study is the tendency for a greater fraction of TCs to make landfall over the U.S. in the warmer climate. This is a key factor associated with the lack of significant change in the frequency of landfalling hurricanes despite the reduction in their basin-wide frequency; it also is associated with an increase in landfalling Category 4-5 hurricanes despite no significant increase in their basin-wide frequency. Thus the increase in fraction of landfalling TCs enhances damage risk for the U.S. according to our simulations. Another recent study (Garner et al. 2021) projected a relative shift in TC activity toward the U.S. in a warming climate.

To explore potential mechanisms for this projected change in TC behavior, Fig. 6 depicts the difference (warm climate minus control) in percent of total TC occurrence days at each grid point. Before computing this difference, the percent occurrence for either warm climate or control is found for each grid point, which sums to 100% separately over both the warm climate and control run maps. The U.S. and near-U.S. coastal regions in all the maps tend to be red-shaded, indicating a robust tendency for a greater fraction of TCs to occur in those areas, and consistent with the increase in the fraction of hurricanes or intense hurricane making U.S. landfall (Fig. 3 e, f).

The above changes in Fig. 6 could be associated with a similar shift in TC genesis. To investigate this, we show in Fig. 7 the difference (warm climate minus control) in the percentage of total TC genesis events occurring at each grid point. This metric tends to show reddish colors near the US, meaning a tendency for TC genesis to occur closer to the U.S. in the warmer climate, but this is not seen in all models (e.g., CCSM3, CM2.0, CM2.1 and MRI show a mix of increases and decreases near the U.S. coast). This particular projected change may be influenced by the TC genesis and track density bias in our modeling framework discussed earlier (Fig. 1). That analysis showed that TC genesis and track density were both excessive off the U.S. East Coast in our control simulations compared to observations. Such a bias is a caveat on further projected increases in such genesis and track density because the projected change has some of the same spatial structure as the bias.

Another possible contributor to the relative increase in TC track density near the U.S. coast is a shift in TC tracks, as would occur with a change in steering flows, for example. To explore this, Fig. 8 shows the change (warm climate minus control) in the vector winds averaged over the 300-850-mb layer. We use this as an approximation for the climatological steering flow that intense TCs in general will experience on average (e.g., Velden and Leslie 1991). The salient feature on these maps are wind anomalies directed from the open Atlantic back toward the U.S. East Coast. This indicates a weakening of the westerly winds that act to recurve hurricanes and tropical storms out to sea and away from the U.S. before they make landfall. Thus, such a change will tend to make U.S. landfalls more likely by weakening the recurvature effect of the westerlies. These easterly anomalies off the U.S. East Coast are a relatively robust feature of the individual CMIP3 models and the CMIP3 and CMIP5 ensembles we examined for the Aug-Oct. season. We have relatively more confidence in this

steering influence than in the increased relative TC genesis near the U.S. East Coast with climate warming because of the robustness of the steering flow change in the CMIP models. Related to these flow changes, projected reductions in vertical wind shear off the U.S. East Coast (K13, their Fig. 9; Ting et al. 2019) may also contribute to the increased TC frequency there.

Returning to the issue of only two models (CMIP3 GFDL CM2.0 and CM2.1) showing statistically significant changes in TC propagation speed, Fig. 8 shows that those two models are distinguished by particularly pronounced easterly anomalies in 300-850 mb averaged vector winds across the tropical Atlantic (10^o - 20^oN). These anomalies imply an increase in the easterly steering flow for TCs moving westward across the tropical Atlantic, which would contribute to increased average propagation speed, although the weakened westerlies at higher latitudes in these and other models would tend to decrease propagation speeds after recurvature.

In short, we have only tentative confidence at this stage in the increase in proportion of TCs making U.S. landfall in our simulations, particularly since the changing TC genesis location factor is one where we have concerns about model biases, while for the steering flow influence we have more confidence based on relatively high model agreement on the wind changes in the climate models we examined.

4.2. Insignificant Change in U.S. Landfalling Hurricane Intensity

While the average maximum lifetime intensity of hurricanes increases for the Atlantic basin as a whole, the increase is not robust for U.S. landfalling hurricanes (Fig. 4 b, d) though the latter is a smaller sample in both space and time. The increase in basin-wide hurricane intensity is consistent with other modeling studies (Knutson et al. 2020). The key mechanism behind this change can be understood as the increase in environmental potential intensity due to greenhouse warming (e.g., Emanuel 1987). In the GFDL Hurricane Model, Tuleya et al. (2016) have shown that the hurricane intensity increase with climate warming depends on a competition between intensification due to higher SSTs, and an offsetting reduction of intensity due to amplified warming of the upper troposphere compared to the surface. They also documented the importance of environmental vertical wind shear for modeled hurricane intensity. Here we review these potential environmental influences on our simulated hurricane intensities. Maps of ensemble mean changes in potential intensity and vertical wind shear for the CMIP3 A1B, CMIP5 Early 21st century, and CMIP5 Late 21st century scenarios have been previously shown in Fig. 9 of K13. Those maps show generally increased potential intensity near the U.S. TC landfalling regions but also increased vertical shear, especially in the Caribbean region, with decreased shear in some regions off the U.S. East Coast. The increased vertical shear would, in a climatological sense, have negative impact on intensities for hurricanes traversing westward toward the U.S. across the western Caribbean and Gulf of Mexico. Ting et al. (2019) have also examined the changes in projected vertical shear and potential intensity near the U.S., noting the reduced vertical shear along the East Coast and enhanced shear in the Caribbean region, the latter being a weakening influence on future Gulf Coast landfalling TCs. We interpret the lack of robust projected change in the intensity of U.S. landfalling TCs overall in our study as resulting from several competing effects, including increased potential intensity and regional-scale changes in vertical shear (which appear particularly important for limiting intensification in Gulf Coast region). Another factor which can influence TC intensity is the change in ocean thermal structure (Huang et al. 2015), although this is currently thought to be of only secondary importance as discussed by Emanuel (2015) and Tuleya et al. (2016).

In summary, we have only tentative confidence that there will be little change in average intensity of U.S. landfalling TCs, owing to the complexity of the problem and the competing influences of several important regionally dependent factors.

4.3. Increase in Frequency of U.S. Landfalling Category 4-5 Hurricanes

The projected increase in U.S. landfalling Category 4-5 hurricane frequency (Fig. 3d) is potentially important for societal impacts, yet the statistical evidence in our experiments is not decisive (with three of 13 models indicating a statistically significant increase and ten of 13 models indicating at least a nominal increase). In addition, only one landfalling Category 4-5 hurricane occurred in our control run (27 seasons) compared with three in observations--a bias which makes the projected increase in the model more difficult to interpret statistically. Yet clearly there in a projected increase in our warm climate runs relative to the control. This results from a number of competing factors. For example, there is a decrease in the basin-wide number of hurricanes, but no significant change in the basin-wide number of Category 4-5 hurricanes. This contrast at the basin-wide scale is presumably due to increased average TC intensity over the basin (K13), and it also implies that the probability of a given hurricane reaching Category 4-5 is projected to increase. However, there is not a robust increase in the average intensity of U.S. landfalling hurricanes (Fig. 4d), nor is there an increase in the total number of U.S. landfalling hurricanes. Apparently, the combined influence of the increase in proportion of hurricanes making U.S. landfall (and the proportion of Category 4-5 hurricanes making U.S. landfall) leads to an increase in total number of U.S. landfalling Category 4-5 storms despite there being no change in the basin-wide number of Category 4-5 hurricanes. Clearly, the multiple factors contributing to the frequency of U.S. landfalling Category 4-5 hurricanes implies that it is a difficult metric to project. Therefore, the projected increase in U.S. landfalling Category 4-5 hurricanes is a change for which we have only tentative confidence at present.

4.4. Increase in TC Precipitation Rates

Although we do not focus on TC rain rates as much as other TC metrics in the present study, here we discuss in some detail the TC rain rate behavior with climate warming over the Atlantic, including revisiting some previous studies that included more detailed analyses of our model framework (e.g., K13) as well other models. The general mechanism producing an increase in TC precipitation rates with climate warming is the increase in tropospheric water vapor content in a warmer atmosphere, together with the moisture convergence mechanism which supplies moisture to a hurricane from its surrounding environment (Wang et al. 2015). K13 (see their Fig. 11) showed that the precipitation rate in the GFDL Hurricane Model increased the most (in percent) near the composite storm's core rainfall region, and was especially large within about 100 km of the storm center. This result influenced our choice of using TC rain rates averaged within 100 km of the storm center as our primary metric for this study. K13 found that the TC rain rate increases were generally at or above the rate at which tropical tropospheric water vapor increases with warming [i.e., about 7% per 1^{o} Celsius rise in SST (Held and Soden 2006)]. In our current study, the 18% increase in 100-km radius averaged rainfall rate also exceeds this Clausius-Clapeyron scaling, as the average tropical Atlantic SST increase is about 1.7^{o}C, giving an expected increase in TC rain rate of 12% from water vapor increase alone, assuming constant relative humidity. Liu et al. (2019) found that increased TC intensity with climate warming can lead to "super-Clausius-Clapeyron" increases in projected TC rain rates. As discussed above, there is some indication in our experiments for increased TC intensities with warming (especially considering basin-wide intensities).

Overall, model-based evidence for a substantial TC rain rate increase with climate warming continues to grow. For example, Reed et al. (2021) modeled substantial increases in rain rates for U.S. landfalling TCs. Considering TC rain rates over the Atlantic Ocean basin (as opposed to U.S. landfalling), Patricola and Wehner (2018), Hill and Lackmann (2011) and several other studies reviewed in Knutson et al. (2020) reported broadly similar sensitivities of TC rain rates to climate warming to those simulated here.

The reasons for the higher percentage increase in TC rain rate for higher-intensity U.S. landfalling hurricanes (discussed in Section 3) remains uncertain, but this finding could be influenced by the relatively small sample size of intense U.S. landfalling TCs in our experiments. Additionally, there is a strong observed relationship between the TC rainfall rate itself and TC intensity at landfall (Tuleya et al., 2007) which could play some role in this behavior.

In short, for TC precipitation at the time of U.S. landfall, our study supports previous findings of an increase in Atlantic basin-wide TC rain rates, with the caveat that the statistical significance and robustness across models is not as high for U.S. landfalling TCs as for basin-wide TCs. Nonetheless, we have--at this stage--relatively high confidence that precipitation rates will increase for U.S. landfalling TCs with 21st century climate warming, based on results presented here as well as other assessments of TC precipitation changes (Knutson et al. 2020).

5. Summary and Conclusions

In this analysis, we explored future projections of U.S. landfalling TCs, examining a large number of cases generated using different climate model projections of large-scale environmental conditions, generally for the late 21st century under the CMIP3 A1B scenario or the CMIP5 RCP4.5 scenario. We examined 13 different sets of projected warmed climate conditions based on 10 individual CMIP3 models or on the multi-model ensemble mean projection from the CMIP3 or CMIP5 models.

A robust projection we simulated was an increase in the proportion of TCs making U.S. landfall. Our analysis suggests that this increase is due primarily to changes in the climatological winds which impacted the large-scale steering by favoring TC movement more toward the U.S. East Coast. These changes in the 300-850 hPa wind were evident in most of the CMIP model or ensemble model environments examined. A second related influence was an increase in the percent of TC genesis occurring near the U.S. East Coast in our warm climate downscaling simulations. However we have less confidence in the robustness of this influence, due to the existence of a positive bias in the frequency of TC genesis in this region in our control simulations.

The increase in proportion of landfalling TCs led to an increase in the number of Category 4-5 hurricanes making U.S. landfall. This increase in Category 4-5 landfalling frequency averaged +390% across the model, with at least nominal increases projected for 10 of 13 models (with no change for the other three models); increases in three of 13 models were statistically significant. This projection, while not definitive, contrasts with the robust decrease in Category 1-5 hurricane frequency projected for the Atlantic basin, the projected decrease in basin-wide PDI, and the lack of significant change in the frequency of U.S. landfalling Category 1-5 hurricanes. While basin-wide hurricane intensity increased, there was little significant change projected for intensity of U.S. landfalling hurricanes. Duration of TCs showed a significant decrease (averaging -13%) while propagation speed showed a slight increasing tendency.

Another robust projection was an increase in the precipitation rate for U.S. landfalling TCs—a signal that averaged 18% considering rain averaged within 100 km of the storm center for all categories of hurricanes. At least near the storm, the change appeared to exceed the Clausius-Clapeyron rate of about 7% per degree Celsius of warming, but the changes overall were not as statistically significant for U.S. landfalling storms as for basin-wide storms. Furthermore, the magnitude of the projected increase was larger in percentage terms for more intense categories of landfalling hurricanes for reasons that were not clear. The limited statistical significance for rain rates of U.S. landfalling TCs at landfall and the increased percentage change of rain rate for higher category TCs may both be related to the relatively limited number of cases available.

There are several important caveats for our study. First, the model framework shows limited skill in simulating the historical year-to-year variability of U.S. landfalling TC activity using SSTs and the NCEP/NCAR Reanalysis as large-scale climate forcings. Excessive TC genesis near to and east of the U.S. East Coast in the control run raises some concerns about projected increases in TC genesis in those regions in the climate change scenarios. There is also uncertainty in the climate change signal in large-scale environmental parameters, which is partly reflected in the spread of results across the different model-derived scenarios. The spread shown in our various results cannot be assumed to represent the true confidence intervals for results in this study. Despite these

limitations, it is important to test our models with such future climate change scenarios and continue to compare modeled scenarios with the growing observational database to work toward a better understanding of the changes in landfalling hurricane risk facing society in the coming decades.

Acknowledgements. We thank the CMIP3 and CMIP5 modeling groups for contributing to the CMIP data base. We thank three anonymous reviewers as well as Hiro Murakami and Tim Marchok from GFDL/NOAA for providing valuable comments to improve our manuscript.

REFERENCES

Bender MA, Knutson TR, Tuleya RE, Sirutis JJ, Vecchi GA, Garner ST, Held IM (2010) Modeled impact of anthropogenic warming on the frequency of intense Atlantic hurricanes. Science 327:5964. DOI:10.1126/science.1180568

Chen JH, Lin SJ (2013) Seasonal predictions of tropical cyclones using a 25-km resolution general circulation model. J Clim 26(2), DOI:10.1175/JCLI-D-12-00061.1.

Colbert AJ, Soden BJ, Vecchi GA, Kirtman BP (2013) The impact of anthropogenic climate change on North Atlantic tropical cyclone tracks. J Clim 26(12): 4088-4095

Dunstone N, Smith D, Booth B, et al (2013) Anthropogenic aerosol forcing of Atlantic tropical storms. Nat Geosci 6:534–539. https://doi.org/10.1038/ngeo1854

Emanuel KA (1987) The dependence of hurricane intensity on climate. Nature 326:483–485. https://doi.org/10.1038/326483a0.

Emanuel KA (2015) Effect of upper-ocean evolution on projected trends in tropical cyclone activity. J Clim 28:8165–8170. https://doi.org/10.1175/JCLI-D-15-0401.1.

Garner AJ, Kopp RE, Horton BP (2021) Evolving tropical cyclone tracks in the North Atlantic in a warming climate. Earth's Future 9: e2021EF002326. https://doi.org/10.1029/2021EF002326

Gori A, Lin N, Xi D, Emanuel K (2022) Tropical cyclone climatology change greatly exacerbates US extreme rainfall-surge hazard. Nat Clim Change 12: 171-178.

Hassanzadeh P, Lee CY, Nabizadeh E, et al (2020) Effects of climate change on the movement of future landfalling Texas tropical cyclones. Nat Comm **11:**3319. https://doi.org/10.1038/s41467-020-17130-7

Hill KA, Lackmann GM (2011) The impact of future climate change on TC intensity and structure: a downscaling approach, J Clim 24(17):4644-4661.

Held IM, Soden BJ (2006) Robust responses of the hydrological cycle to global warming, J Clim 19(21):5686-5699.

Hsieh TL, Vecchi G, Yang W, Held I, Garner S (2020) Large-scale control on the frequency of tropical cyclones and seeds: a consistent relationship across a hierarchy of global atmospheric models. Clim Dyn 55:3177-3196.

Huang P, Lin II, Chou C, Huang RH (2015) Change in ocean subsurface environment to suppress tropical cyclone intensification under global warming. Nat Comm 6:7188. https://doi.org/10.1038/ncomms8188.

Kalnay E et al (1996) The NCEP/NCAR 40-year re-analysis project. Bull Am Meteorol Soc **77:**437–471.

Klotzbach PJ et al (2020) Surface pressure a more skillful predictor of normalized hurricane damage than maximum sustained wind. Bull Am Meteorol Soc 101(6):E830-E846. doi:10.1175/BAMS-D-19-0062.1

Knapp KR, Kruk MC, Levinson DH, Gibney EJ (2009) Archive compiles a new resource for global tropical cyclone research. Eos Trans AGU 90. doi:10.1029/2009EO060002.

Knutson T et al (2020) Tropical cyclones and climate change assessment: Part II: Projected response to anthropogenic warming. Bull Am Meteorol Soc 101(3):E303-E322.

Knutson TR, Sirutis JJ, Garner ST, Held IM, Tuleya RE (2007) Simulation of the recent multidecadal increase of Atlantic hurricane activity using an 18-km-grid regional model. Bull Am Meteorol Soc 88(10). DOI:10.1175/BAMS-88-10-1549.

Knutson TR, Sirutis JJ, Vecchi G, Garner ST, Zhao M, Kim HS, Bender MA, Tuleya RE, Held IM, Villarini G (2013) Dynamical downscaling projections of 21st century Atlantic hurricane activity: CMIP3 and CMIP5 model-based scenario. J Clim 26(17). DOI:10.1175/JCLI-D-12-00539.1.

Knutson T, Sirutis JJ, Zhao M, Tuleya R, Bender M, Vecchi G, Villarini G, Chavas D (2015): Global projections of intense tropical cyclone activity for the late 21st century from dynamical downscaling of CMIP5/RCP4.5 scenarios. J Clim 28(18), DOI:10.1175/JCLI-D-15-0129.1

Kossin, J., 2017: Hurricane intensification along United States coast suppressed during active hurricane periods. Nature 541:390–393. https://doi.org/10.1038/nature20783

Kossin JP (2019) Reply to: Moon, I.-J. et al.; Lanzante, J. R. Nature 570**:**E16–E22. https://doi.org/10.1038/s41586-019-1224-1.

Levin EL, Murakami H (2019) Impact of anthropogenic climate change on United States major hurricane landfall frequency. J Mar Sci Eng 7:135. https://doi.org/10.3390/jmse7050135

Liu M, Vecchi GA, Smith JA, Knutson TR (2019) Causes of large projected increases in hurricane precipitation rates with global warming. npj Clim Atmos Sci 2:38. https://doi.org/10.1038/s41612-019-0095-3

Liu M, Vecchi GA, Smith JA, Murakami H (2018). Projection of landfalling–tropical cyclone rainfall in the eastern United States under anthropogenic warming. J Clim 31(18): 7269-7286.

Murakami H, Delworth TL, Cooke WF, Zhao M, Xiang B, Hsu PC (2020): Detected climatic change in global distribution of tropical cyclones. Proc Nat Acad Sci 117(20):10706-10714. DOI: 10.1073/pnas.1922500117

Murakami H, Vecchi GA, Villarini G, Delworth TL, Gudgel R, Underwood S, Yang X, Zhang W, Lin SJ (2016) Seasonal forecasts of major hurricanes and landfalling tropical cyclones using a high-resolution GFDL coupled climate model. J Clim 29:7977-7989.

Murakami H, Wang B (2010) Future change of North Atlantic tropical cyclone tracks: projection by a 20-km-mesh global atmospheric model, J Clim, 23(10):2699-2721.

Patricola CM, Wehner MF (2018) Anthropogenic influences on major tropical cyclone events. Nature 563: 339–346. https://doi.org/10.1038/s41586-018-0673-2

Pielke RA Jr, Gratz J, Landsea CW, Collins D, Saunders MA, Musulin R (2008) Normalized hurricane damage in the United States: 1900–2005. Nat Hazards Rev 9:29. https://doi.org/10.1061/(ASCE)1527-6988(2008)9:1(29).

Reed KA, Wehner MF, Stansfield AM, Zarzycki CM (2021) Anthropogenic influence on Hurricane Dorian's extreme rainfall. [in "Explaining Extremes of 2019 from a Climate Perspective"]. Bull Am Meteorol Soc 102(1):S9–S15, https://doi.org/10.1175/BAMS-D-20-0160.1.

Stansfield AM, Reed KA, Zarzycki CM (2020) Changes in precipitation from North Atlantic tropical cyclones under RCP scenarios in the variable-resolution community atmosphere model. Geophys Res Lett 47: e2019GL086930. https://doi.org/10.1029/2019GL086930

Ting M, Kossin JP, Camargo SJ et al (2019) Past and future hurricane intensity change along the U.S. East Coast. Sci Rep 9:7795. https://doi.org/10.1038/s41598-019-44252-w

Tuleya RE, Bender M, Knutson TR, Sirutis JJ, Thomas B, Ginis I (2016) Impact of upper-tropospheric temperature anomalies and vertical wind shear on tropical cyclone evolution using an idealized version of the operational GFDL hurricane model. J Atm Sci *73*(10):3803-3820.

Tuleya R, DeMaria M, Kuligowski RJ (2007) Evaluation of GFDL and simple statistical model rainfall forecasts for U.S. landfalling tropical storms. Wea Forecasting 22:56–70, doi:10.1175/WAF972.1.

Velden CS, Leslie LM (1991) The basic relationship between tropical cyclone intensity and the depth of the environmental steering layer in the Australian region. Wea Forecasting 6(2): 244-253.

Wang CC, Lin BX, Chen CT, Lo SH (2015) Quantifying the effects of long-term climate change on tropical cyclone rainfall using a cloud-resolving model: examples of two landfall typhoons in Taiwan. J Clim 28:66–85, https://doi.org/10.1175/JCLI-D-14-00044.1.

Wright D, Knutson TR, Smith JA (2015) Regional climate model projections of rainfall from U.S. landfalling tropical cyclones. Clim Dyn 45:3365-3379. DOI:10.1007/s00382-015-2544-y.

Vecchi GA, Knutson TR (2008) On estimates of historical North Atlantic tropical cyclone activity. J Clim 21(14), DOI:10.1175/2008JCLI2178.1.

Vecchi, G. A., and T. R. Knutson, 2011: Estimating annual numbers of Atlantic hurricanes missing from the HURDAT database (1878-1965) using ship track density. J Clim 24(6):1736-1746. DOI:10.1175/2010JCLI3810.1.

Vecchi GA, Landsea C, Zhang W, Villarini G, Knutson TR (2021) Changes in Atlantic major hurricane frequency since the late-19th century. Nat Comm 12:4054, DOI:10.1038/s41467-021-24268-5.

Yan X, Zhang R, Knutson TR (2017) The role of Atlantic overturning circulation in the recent decline of Atlantic major hurricane frequency. Nat Comm 8:1695. https://doi.org/10.1038/s41467-017-01377-8

Zhang G, Murakami H, Knutson TR, Mizuta R, Yoshida K (2020) Tropical cyclone motion in a changing climate**.** Sci Adv*,* 6(17):eaaz7610, DOI:10.1126/sciadv.aaz7610.

Zhao M, Held IM, Lin SJ, Vecchi GA (2009) Simulations of global hurricane climatology, interannual variability, and response to global warming using a 50km resolution GCM. J Clim 22(24), DOI:10.1175/2009JCLI3049.1

FIGURES

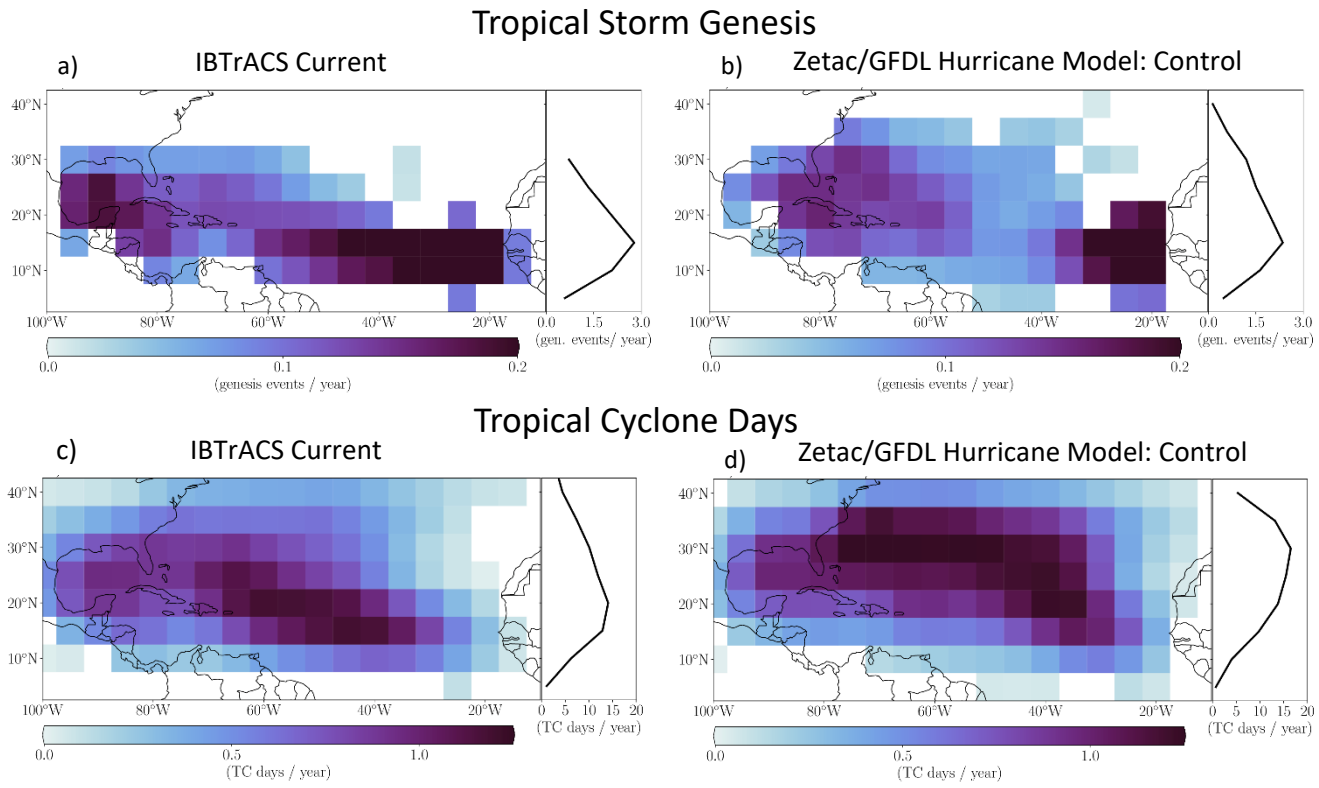

Fig. 1. Distribution of tropical storm genesis locations (a, b) in events per year and tropical cyclone (TC) track density (c, d) in TC days per year based on IBTrACS observations (a, c) and downscaled simulations. The downscaled simulations use the NCEP Reanalysis to provide the initial conditions, boundary conditions and the target for the large-scale interior spectral nudging for the initial Zetac model Control (present day) simulations. The storms from Zetac model were further downscaled (individually by storm) using the GFDL Hurricane model. Observations and models cover the months of Aug-Oct. for the years 1980-2016. The insets along the right edge of each panel show the zonally accumulated value for each row of grid points (or latitude row) on the map.

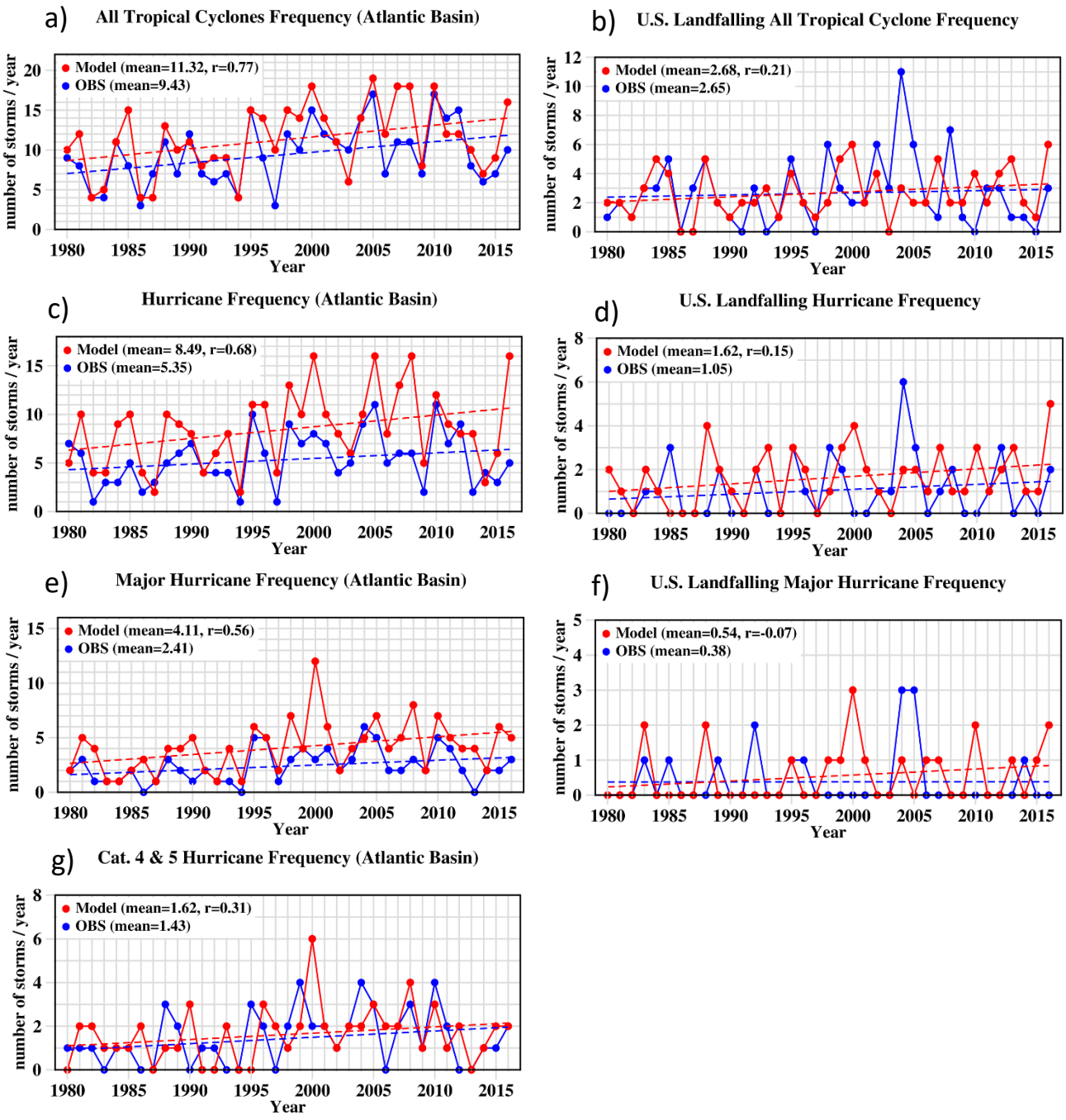

Fig. 2. Annual (Aug.-Oct.) counts of Atlantic basin-wide (a, c, e, g) and contiguous U.S. landfalling (b, d, f) tropical cyclones in observations (blue) or as simulated in the downscaling framework using NCEP Reanalysis large-scale forcing. Intensity categories are: a,b) tropical storm and higher; c,d) Category 1-5 hurricanes; e,f) Major (Category 3-5) hurricanes; or g) very intense (Category 4-5) hurricanes. The series means and correlations (r) between observed and modeled series are shown in each panel. Dashed lines are linear trends. Differing y-axis scaling is used.

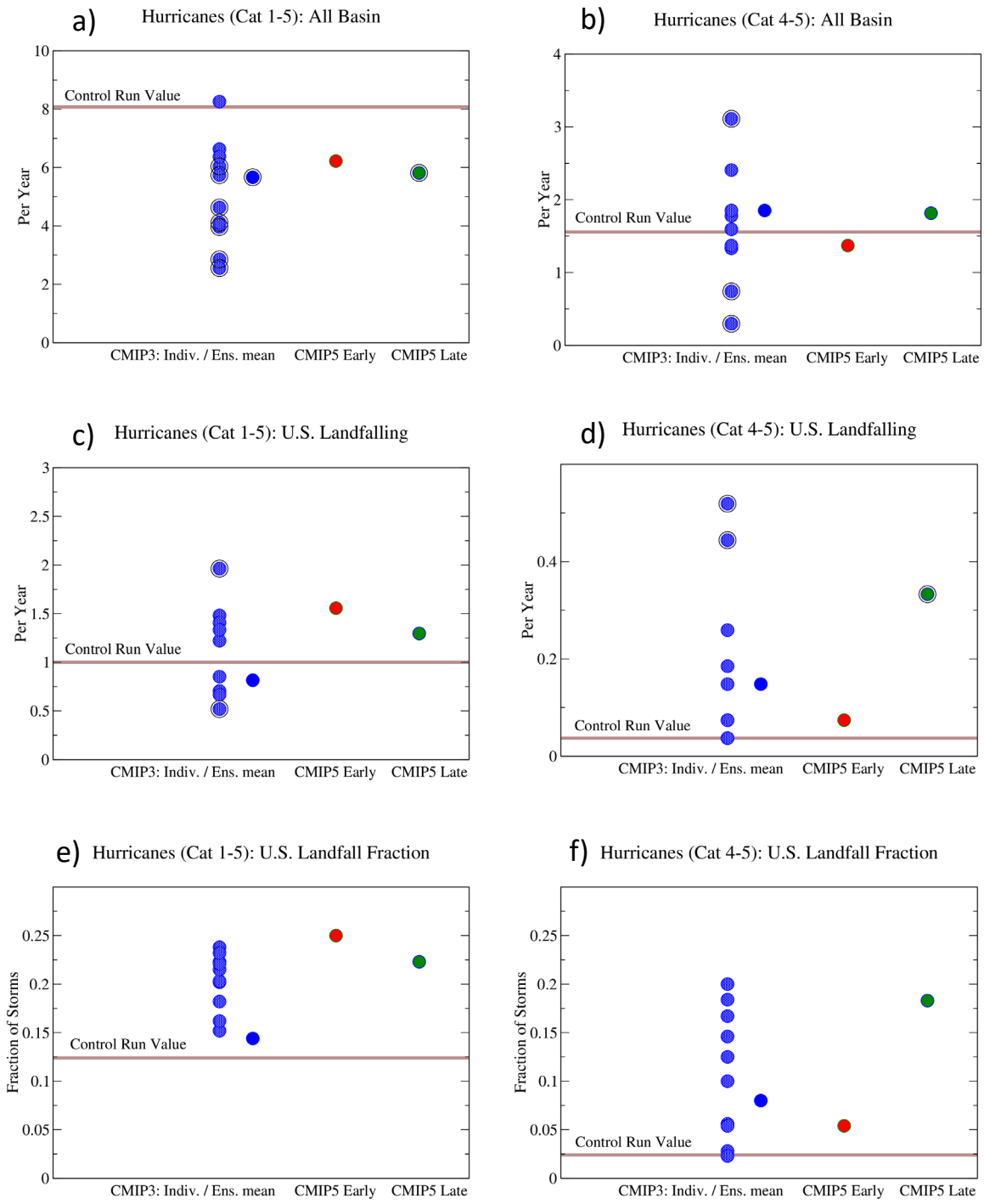

Fig. 3. Summary comparison of hurricane activity measures for the Control (present day, thick line) and CMIP3 or CMIP5 warming climate scenarios (see x-axis labels). In panels a-d the average number of storms per year of a given storm type is shown for: Atlantic basin-wide a) Category 1-5 or b) Category 4-5 hurricanes, and for U.S. landfalling c) Category 1-5 or d) Category 4-5 hurricanes. Panels e,f show the fraction of storms making U.S. landfall for e) Category 1-5 or f) Category 4-5 hurricanes. The slightly larger "ringed" dots denote statistically significant changes according to a Mann-Whitney test.

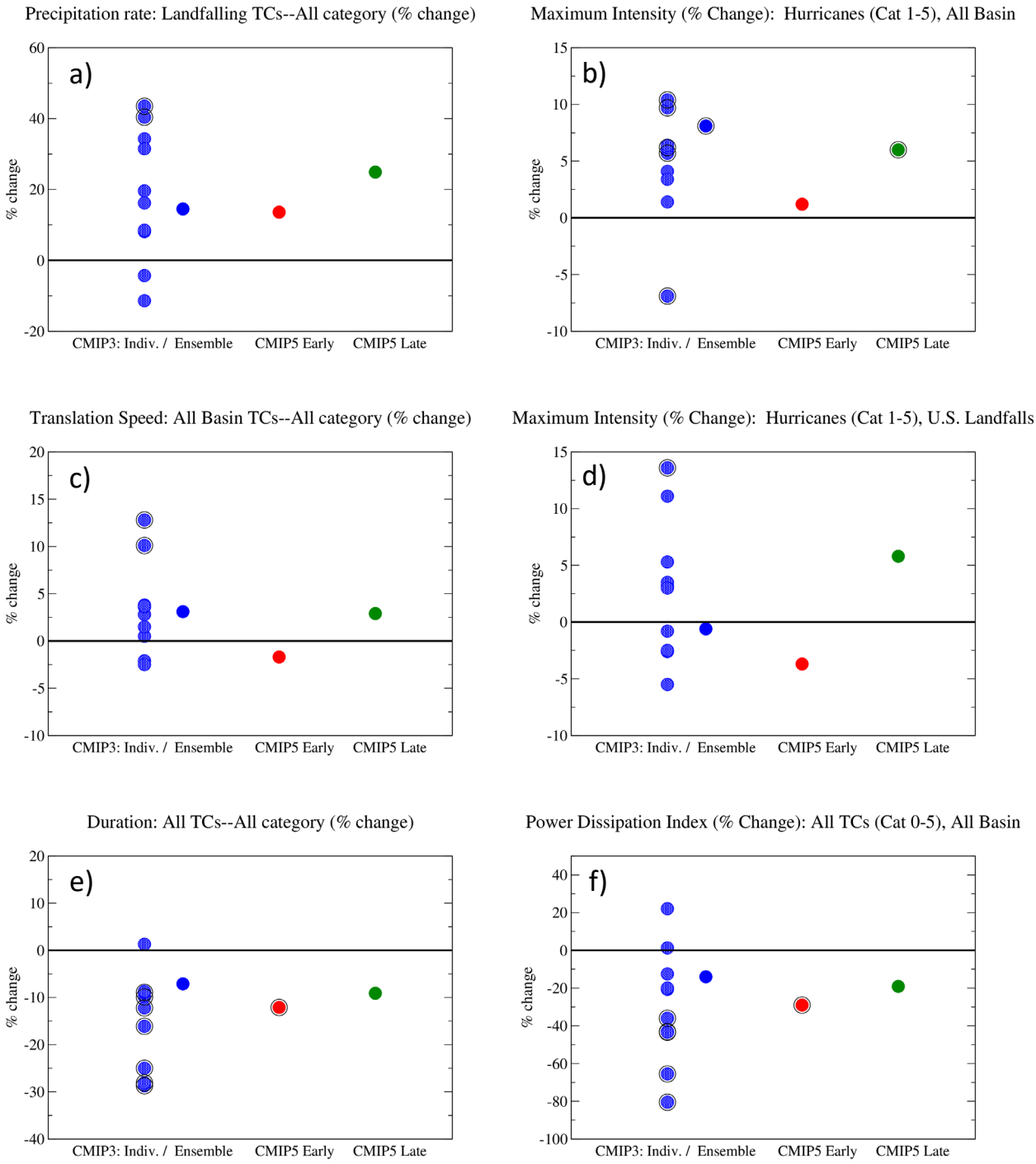

Fig. 4. Summary comparison of hurricane activity measures for the Control (present day) and CMIP3 or CMIP5 warming climate scenarios (see x-axis labels). For each panel the percentage change (from present-day to warm climate scenario) in the given TC metric is shown. The slightly larger "ringed" dots significant statistically significant changes according to a Mann-Whitney test (see Table 1 in Appendix). Metrics include percent changes in: a) precipitation rate for U.S. landfalling TCs (within 100 km of the TC center); b) lifetime maximum 10 m wind speed intensity of Atlantic basin hurricanes; c) basin-wide average TC translation speed; d) maximum intensity (10 m wind speeds) at or just prior to U.S. landfall; e) basin-wide average TC duration; and f) TC basin-wide power dissipation index. See main text and Supplemental Material (Table 1) for further details.

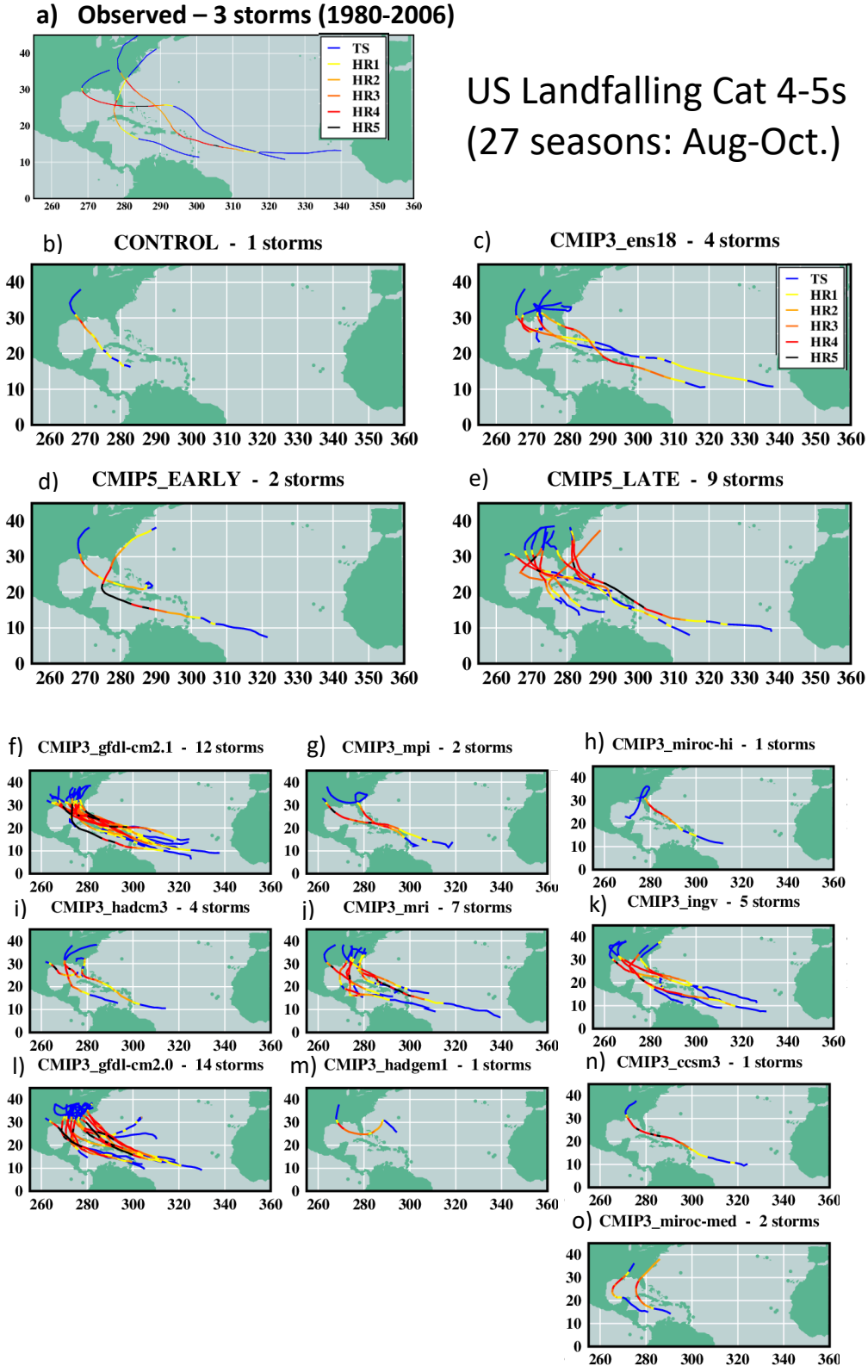

Fig. 5. Tracks of all tropical cyclones that made U.S. landfall while at Category 4 or 5 intensity based on: a) observations or b) NCEP Reanalysis-driven present-day simulations (Control) for Aug-Oct. of the years 1980-2006. The remaining simulation panels used the reanalysis variability from 1980-2006 while their mean climate conditions were altered from the reanalysis according to warming scenarios derived from: c) CMIP3 18-model ensemble (late 21st century A1B scenario); d, e) CMIP5 multi-model ensemble early (d) and late (e) 21st century RCP4.5 scenarios; or f-o) individual CMIP3 models. See text for details.

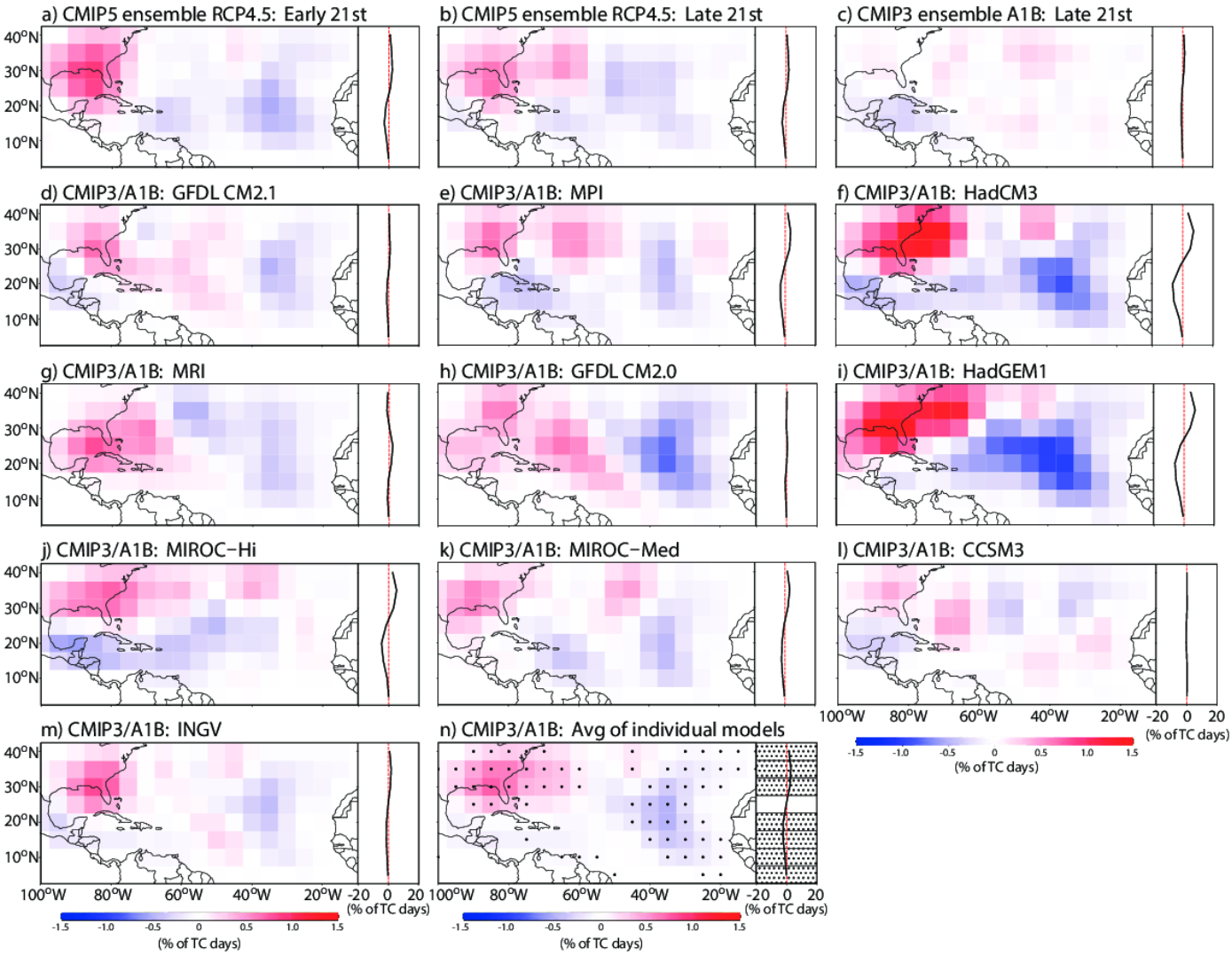

Fig. 6. Each panel shows the difference in percentage of total TC days occurring at each grid point between the warm climate and control climate (warm minus control). In panel (n) the average of the 10 individual CMIP3 model results is shown, with dots where results from 8 or more of the 10 individual CMIP3 models agree on the sign of change. The insets along the right edge of each plot (a-n) show the difference between the zonal accumulated values for the warm climate runs minus those of the control run.

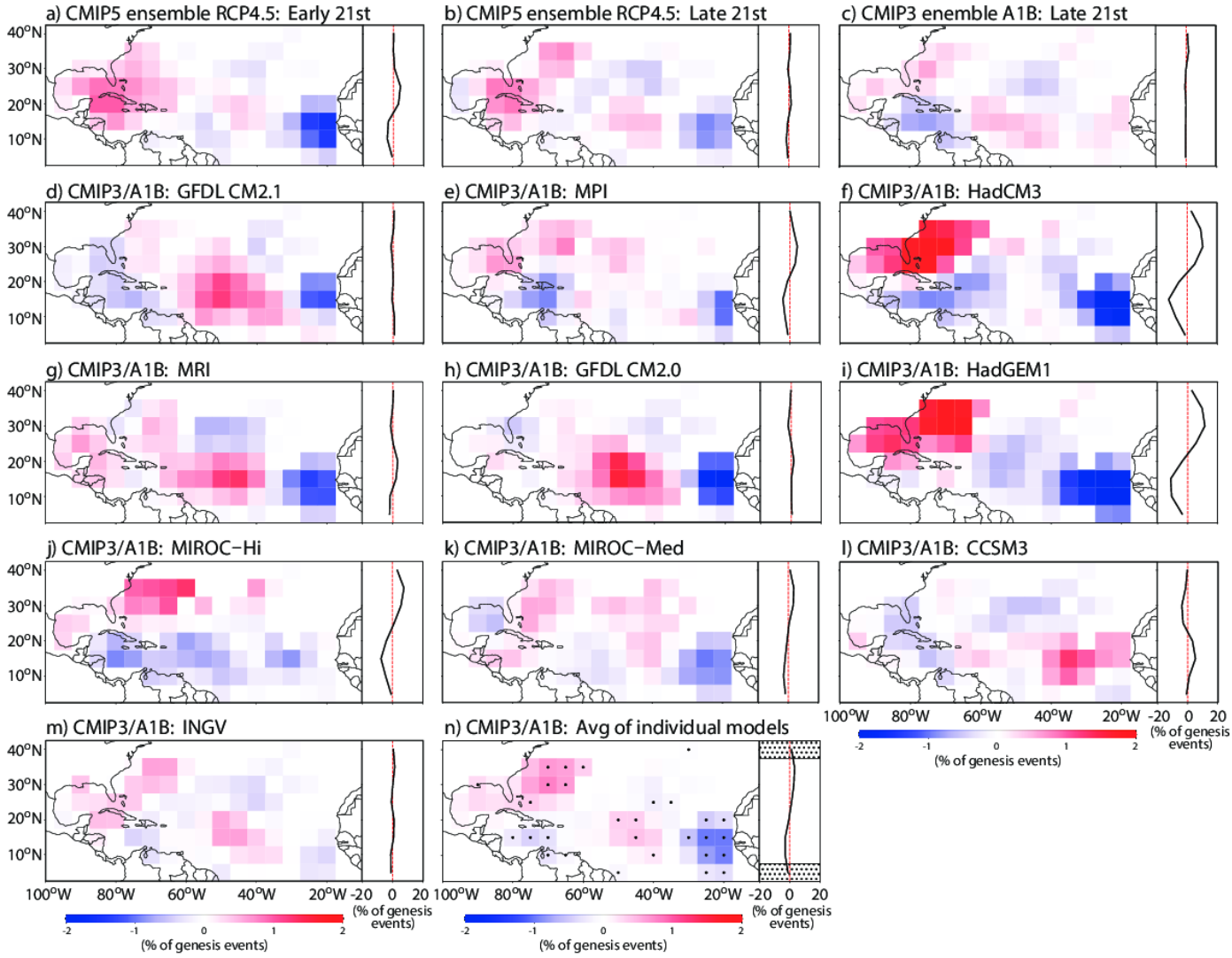

Fig. 7. Each panel shows the difference in the percentage of total TC genesis events occurring at grid point, with the difference taken between the warm climate and control climate maps (warm minus control). In panel (n) the average of the 10 individual CMIP3 model results is shown, with dots where results from 8 or more of the 10 individual CMIP3 models agree on the sign of change. The insets along the right edge of each plot (a-n) show the difference between the zonal accumulated values for the warm climate runs minus those of the control run.

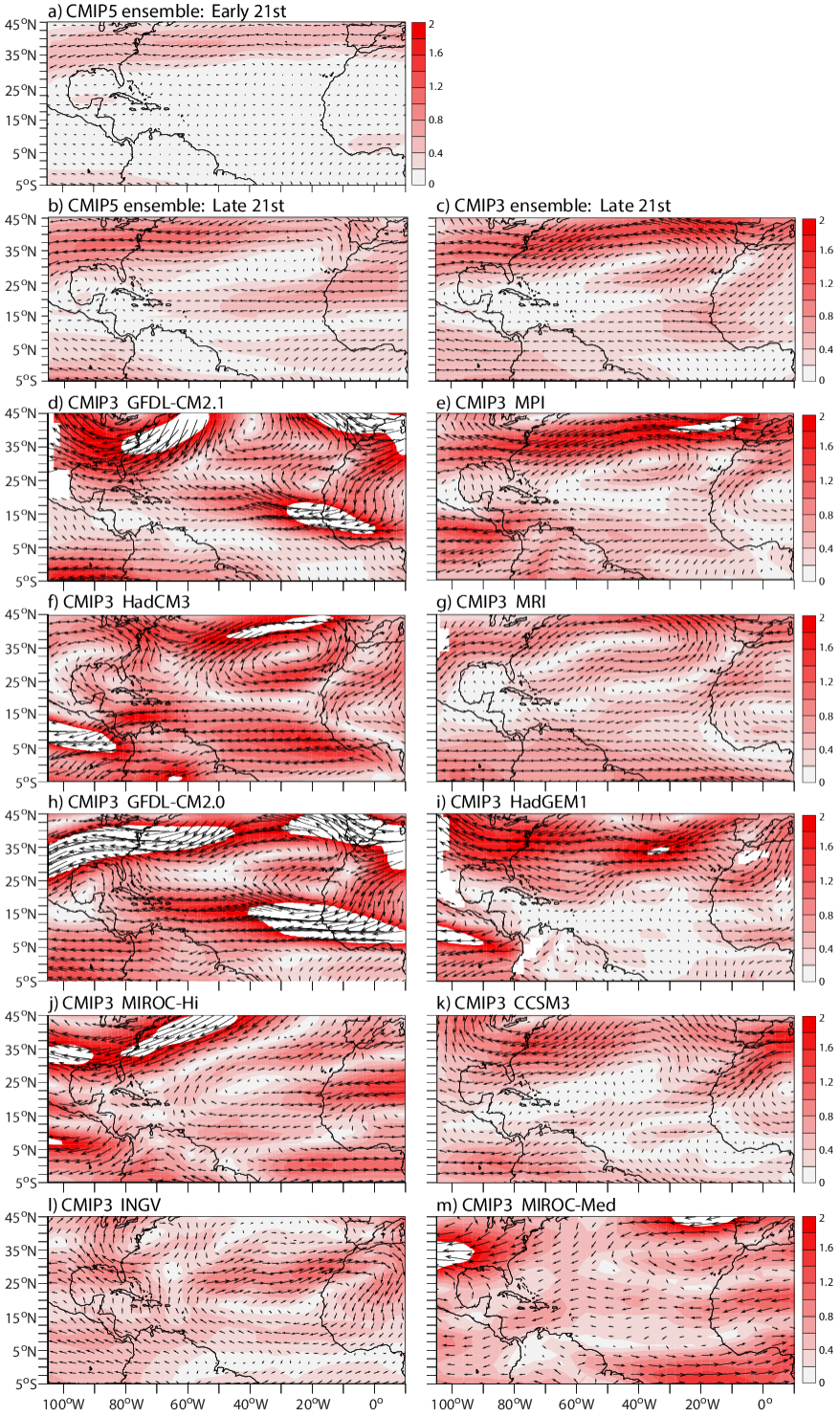

Fig. 8. Change (warm climate minus control) in the climatological average of the vector winds in the 300-850mb layer. This is an approximate indicator of the change in steering flow that TCs on average would experience. Panel titles identify the model or model ensemble shown. Solid white shading: magnitudes exceeding 2 m s^{-1}.

SUPPLEMENTAL MATERIAL:

Dynamical downscaling projections of late 21st century U.S. landfalling hurricane activity

Mar. 30, 2022 version

Climatic Change (in press)

This supplemental material contains a detailed Methodology section and Table 1, which is a detailed series of TC metrics and their response to climate change as discussed in the main text.

1. METHODOLOGICAL DETAILS

1.1 Overview

Our study explores 21st century climate change projections for U.S. landfalling hurricane activity using a two-step dynamical downscaling framework, together with tropical climate change projections from multiple CMIP3 and CMIP5 climate models-- the same models as used in K13. In addition to the present-day runs, 13 CMIP3 or CMIP5 climate change scenarios were explored.

In the earlier study, the highest resolution simulations with the GFDL hurricane model (i.e., the second step of our two-step downscaling procedure) were limited to five days in length, as we were closely following the procedures of the operational GFDL hurricane model from that time period, which had some operational limitations. Specifically, in Knutson et al. (2013; hereafter K13) each five-day downscaling case was started from initial conditions, obtained from the 18 km grid Zetac regional atmospheric model (Knutson et al. 2007; hereafter K07), beginning two days prior to the storm's time of maximum intensity as simulated in the Zetac model. The Zetac model simulated hurricanes only up to about 50 m s^{-1} intensity in terms of surface wind speed, which was one reason why the second downscaling step using the higher-resolution GFDL hurricane model (with 9 km spacing for the inner grid) was necessary. In contrast, in the present study, we wish to focus on the U.S. landfalling stages (meaning here landfalling for the Contiguous U.S., i.e., excluding Hawaii, Puerto Rico, Guam, etc.). We also focus, using higher resolution, on simulating realistic storm intensity and structure throughout each storm's life cycle. We initialize each high-resolution hurricane model simulation (storm case) using initial conditions from the regional Zetac model at the time when tropical storm intensity of 17.5 m s^{-1} is first reached in the Zetac model, and then integrate the hurricane model forward for 15 days.

The methodology for our study mostly follows that in K13, K07, and Bender et al. (2010), and is described in detail in those studies. Here the methodology is presented only in abbreviated form, where we focus mainly on aspects of the methodology that differ from K13 and K07. The reader is referred to these previous studies for further details.

1.2 Experimental Design for Present-day Hurricane Simulations

The simulation of Atlantic hurricanes proceeds in in several stages. We performed control (present-day) and climate change simulations for 27 seasons (1980-2006, and modified "warm-climate" versions of the 1980-2006 seasons). Before we perform climate change simulations, we first want to assess how well our complete modeling system is able to simulate Atlantic hurricane activity and its interannual variability for a given set of environmental conditions. To explore this, we first test our system by initializing and forcing it with present-day large-scale climate conditions as defined by the time-evolving NCEP/NCAR Reanalysis I (Kalnay et al. 1996) of the atmosphere and observed sea surface temperatures (SSTs). Because during our projected we decided that we wanted more robust statistics for the correlations between simulated and observed interannual variability, we expanded the years of our control simulation through 2016 (i.e., 1980-2016), though not the entire analysis, which was much more computationally expensive. In a few cases, intermediate ending year results are presented here (i.e., 1980-2013).

For each year analyzed (e.g., 1980-2016), we simulate the three-month period August-October with the regional 18-km grid Zetac regional model, using the reanalysis to provide lateral boundary conditions, the atmospheric initial conditions, and the time-evolving target fields for interior spectral nudging of the very large scale (zonal and meridional wavenumber 0-2 of the regional domain) atmospheric environment, with a nudging timescale of 12 hours. Note that since only the large-scale atmospheric conditions are used as our interior spectral nudging target a high-resolution atmospheric analysis is not required for the nudging.

The simulations were limited to the peak three months of the Atlantic TC season (Aug. – Oct.) to save on computation requirements, which may introduce some uncertainty to our results, particularly if aspects of seasonality, such as the length of the Atlantic TC season, were to change with climate warming. For example, Dwyer et al. (2015) find that in model projections, models that project fewer TCs with climate warming also simulate shorter seasons, and vice versa for models projecting more TCs. This potential limitation of our Aug.-Oct. season approach should be kept in mind in interpreting our results. The model was run over specified time-evolving SSTs. The Zetac regional model is a nonhydrostatic model run here without convective parameterization (see K07 for details).

Tropical storm cases are identified in these three-month simulations using the automated TC search procedure described in K07, including a requirement for warm-core structure, surface wind speeds for the storm feature of at least 17.5 m s^{-1}, and total duration of at least 48 hours (not necessarily consecutive hours) at an intensity of at least 17.5 m s^{-1}. Landfalling TCs for the Contiguous U.S. (CONUS) were defined by the intersection of the surface center of the TC (defined by the minimum in surface pressure) with the coastline (https://www.nhc.noaa.gov/aboutgloss.shtml), where the land region was defined as the 48 contiguous states (excluding Alaska and Hawaii). Multiple CONUS landfalls by a single storm were counted as separate landfalls in our statistics.

Each individual tropical storm case from the Zetac regional model was then re-run as an individual 15-day case study using the GFDL Hurricane Model. The GFDL Hurricane Model is a high-resolution coupled regional prediction model that was used operationally by the National Weather Service (NWS) from 1995 (Bender et al. 2007; 2010) until it was retired from operations in 2017. The version used in this study was the model used in Bender et al. (2010), which was the version that was operational from 2006 through 2010. The model consists of a triply nested moveable mesh system designed for hurricane track and intensity prediction, and has grid-spacing of about 8.5 km in the innermost 5^{o}x5^{o} nest. The GFDL Hurricane Model cases are initialized at the time a given tropical storm (see criteria above) first reaches tropical storm strength, as opposed to being initialized after it has reached at least 48 hours duration at tropical storm strength. About 13% of tropical storm genesis events identified in the Zetac regional model failed to survive and develop as storms after being initialized into the GFDL Hurricane Model. In those cases, we attempted to restart the case using initial conditions from six hours later in the Zetac simulation, and in most cases (about 70% of such cases) the storms did survive and were tracked. If, after this second attempt, a storm case still failed to survive even a few timesteps in the model, the case was discarded and was not counted as a genesis event or further analyzed in our GFDL Hurricane Model analyses. About 4% of Zetac tropical storm genesis cases were discarded for this reason.

The atmospheric component of the GFDL Hurricane Model has been coupled to the Princeton Ocean Model since 2001 (Bender et al. 2007) and for the present-day simulations uses a realistic present-day climatology of ocean subsurface temperature and salinity (U.S. Navy GDEM, or Generalized Digital Environmental Model) so that the hurricane model is able to simulate a realistic ocean response to the strong hurricane forcing, including generation of a "cold wake" in the SST field as it passes over the ocean (Bender et al. 2007). Following the procedure used operationally (2006-2010) for storm initialization, the ocean model state for each storm case was initialized by running the ocean model for two days using the GDEM climatology values for ocean temperature and salinity with SSTs prescribed. During this first step, a sharpening technique is employed in order to assimilate a reasonable climatologically based Loop Current and Gulf Stream ocean structure (Yablonsky et al. 2015). Next, starting three days prior to the storm case start date, atmospheric forcing is imposed, based on the model's storm wind field. In this second step, the SSTs as well as ocean temperatures and salinity are allowed to evolve. This procedure is used to initialize the cold wake in the SST and ocean temperature field due to the passage of the storm. A limitation of the version of the operational GFDL Hurricane Modeling System used in this study was that the dynamical ocean domain did not cover the full North Atlantic basin but rather the coupled model used two separate ocean model domains—one covering the central to eastern Atlantic and the other the central to western Atlantic (see Fig. 5 of Bender et al. 2007). Therefore, storms traversing the central Atlantic could run off one of these grids and lose their ocean coupling. However since the two ocean grids were overlapped, when this occurred, we restarted the storm on the second ocean grid before the coupling was lost and then continued the simulation with full ocean coupling until landfall. Since this happened only for a small subset of runs, and the transition occurred very far from U.S. landfall, and was treated the same for both present-day and warm climate experiments, we believe that this limitation of our model framework was very unlikely to affect our overall conclusions.

In addition, during the 15-day integrations, the time-mean state of the atmospheric fields in the GFDL Hurricane Model tended to drift from the initial state (taken from the Zetac model) toward the GFDL Hurricane Model's climatological state, which differed from that of the host (Zetac) regional model. However, the average drift that occurred was found to be similar for present-day climate and future warm climate scenarios, so that any systematic effects of the drift on the storm characteristics should be similar in the present-day and warm climate cases. Therefore the drift should have little influence on the modeled TC climate change responses.

1.3 U.S. landfalling TC tracks: Zetac model vs. GFDL Hurricane Model

To illustrate some of the basic simulation characteristics of storms in the Zetac regional model vs. the GFDL Hurricane Model, Fig. S1 compares the tracks and intensities of simulated U.S. landfalling TCs from the two modeling systems for the years 1980-2013. The tracks from the higher resolution model resemble those of from the Zetac regional model, although the intensities clearly extend to higher categories (up to category 5) in the hurricane model compared to the Zetac model, as expected due to the coarser resolution of the Zetac model. Almost no track segments above category 1 are found in the Zetac regional model simulations. This illustrates the basic advantage of including the second downscaling step into the GFDL Hurricane Model: to simulate TCs with intensities higher than category 1 (see also Bender et al. 2010 and K13). The remaining figures and analyses in this report are based on the GFDL Hurricane Model simulations.

Figure S1 also shows that the tracks in the Zetac regional model do not extend poleward of about 43°N while tracks terminate even further south (near 38°N) in the GFDL Hurricane Model simulations. These track truncation effects, which can affect the duration of storms, are due to the presence of the Zetac regional model boundary at 45°N and the difference in each model's structure and tracking algorithm. In the Zetac model tracks typically end as storms decay as they approach the model's boundary. In addition to these limitations, the GFDL model tracks terminate further from the boundary than the Zetac model's storms due to the interaction of the model's

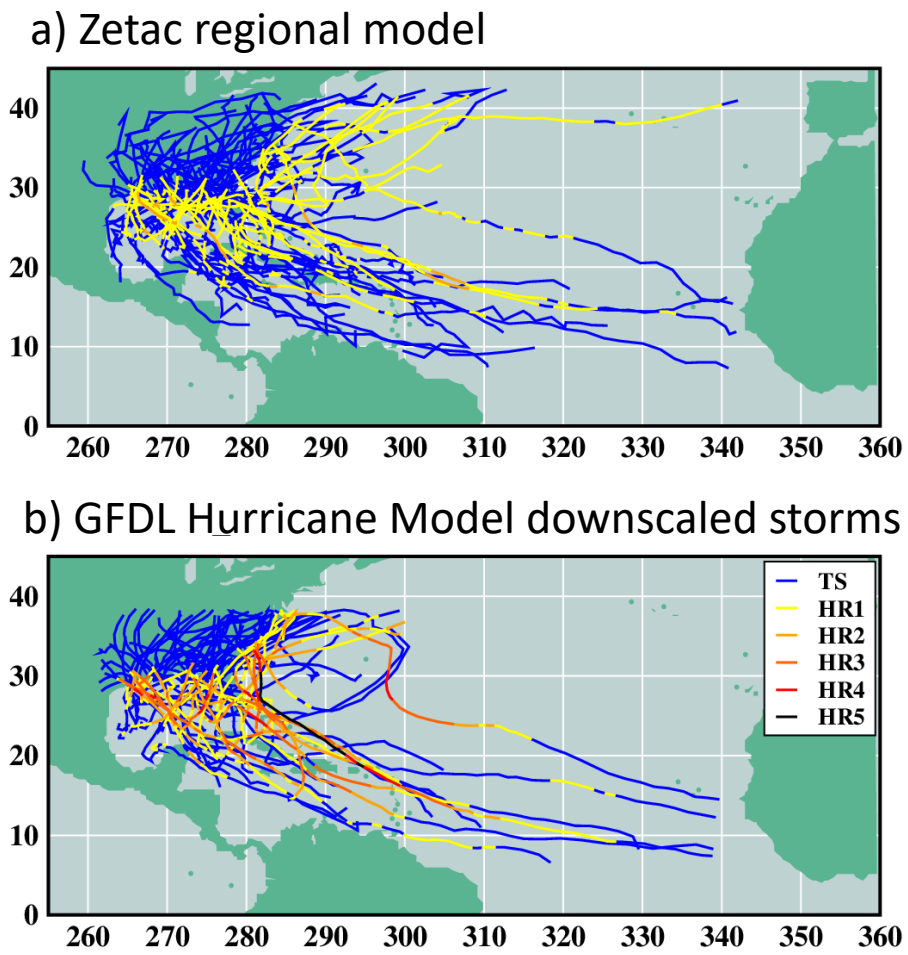

Fig. S1. U.S. landfalling tropical storms and hurricanes for the years 1980-2013 as simulated by: a) the Zetac regional model based on initial conditions, boundary conditions, and large-scale interior spectral nudging targets derived from the NCAR/NCEP Reanalyses for Aug.-Oct. seasons; and b) the GFDL hurricane model using all tropical storm genesis cases from the Zetac regional model (both landfalling and non-landfalling cases in Zetac) as initial conditions and boundary conditions for higher-resolution downscaled simulations, but plotting only contiguous U.S. landfalling hurricane model cases.

moveable nests with the outer boundary; storms cannot be tracked in the GFDL model closer than within about 7^{o} of the model outer boundary partly due to restrictions on the movement of the nested grids.

The observed tropical storm genesis points and tropical storm tracks from IBTrACS s in Fig. 1 of the main text are based on the official Best Track data from the National Hurricane Center. Model tropical storm genesis occurrences are determined from the Zetac regional model runs (except for storms which failed to run even 6 simulated hours in the hurricane model), and are based on the tropical storm identification scheme described above. The identification scheme includes requirements for a warm core, surface wind speed intensity, and duration model (i.e., 48 hours duration—not necessarily consecutive--with tropical warm core characteristics and intensity of at least 17.5 m s^{-1}) in the Zetac regional. The storms that were simulated in the GFDL hurricane model were not further tested for warm core characteristics, but were classified hurricanes of various categories if the surface wind speeds reached the required thresholds.

1.4 Details of Construction of Climate Change Downscaling Simulations

Following on the above-mentioned present-day simulations and analysis of Atlantic hurricane seasons using our two-step downscaling simulations, we next analyze similar sets of experiments, but this time applying a set of climate change conditions. We focus here on 27 seasons (1980-2006) for computational efficiency.

We first created a series of climate change "delta" fields, which we added to the NCEP/NCAR Reanalysis, to create a series of warm-climate perturbation experiments that use realistic conditions (i.e., the reanalysis) as the baseline case. Specifically, we use changes in SST, surface pressure, air temperature, relative humidity, and winds to modify the NCEP/NCAR reanalysis fields that are used as boundary forcing and as the nudging target for the interior spectral nudging procedure with the Zetac regional model. As described in K13, for CMIP3 models, these perturbations included an 18-model ensemble average perturbation (models listed in K13), which was the August-October average of 2081-2100 minus 2001-2020 for the Special Report on Emission Scenarios A1B (SRES A1B) scenario. Then for each of the 10 individual CMIP3 models used in this study (identified in the figures of this study), we created individual model climate change perturbation fields. For this, we first computed the linear trend of each model's data for the period 2001-2100. We then projected this linear trend through time to compute an effective "linear trend difference" between the 2081-2100 period and the 2001-2020 baseline period. Our experimental design re-uses the observed interannual variability from the NCEP/NCAR Reanalysis for the climate change experiments, which is an assumption that the interannual variability of these fields does not change with climate change. We chose this assumption because projected changes in interannual variability of these fields are generally assessed as having less confidence than changes in the large-scale time-mean environmental fields, although this implies some additional uncertainty for our TC projections. We constructed two 18-model ensemble-mean CMIP5 model warm-climate scenarios using the 2016-2035 (early 21st century) or 2081-2100 (late 21st century) period of the CMIP5 RCP4.5 scenario versus the baseline period of 1986-2005 of the CMIP5 historical runs (see K13 for a list of the 18 models). The global temperature difference between present-day and the warm-climate condition was 1.69^{o}C for CMIP3 vs. 1.70^{o}C for the CMIP5 late-21st century case. In sensitivity experiments, we found that hurricane model intensity changes in the warm climate scenarios were relatively insensitive to the small increase in the ocean subsurface vertical temperature gradients associated with the SST warming scenarios (see also Tuleya et al. 2016). Therefore, following Knutson et al. (2013) for the ocean subsurface temperature profiles in the warm climate runs, we used the 18-model ensemble average three-dimensional ocean structure

change from the CMIP3 models to represent the change in ocean temperature stratification in the warmer climate for all of the hurricane model climate change experiments in this study.

2. DETAILED MODELED RESPONSE OF TC METRICS TO CLIMATE WARMING

Details of the simulated response of various TC metrics to the climate warming experiments are presented in Table 1. Key results from Table 1 are summarized and discussed in the main text (Fig. 3 and 4). In Table 1, to focus on results from our experiments where most models agree on the sign of the projected changes, we examine both the level of agreement across the models for projected changes for a given metrics, along with statistical significance test indicators for the individual model results. Mann-Whitney statistical tests for differences in means were performed, assuming that the 27 separate seasons (years) are independent samples. Using this summary approach, Table 1 (and Figs. 3 and 4 or the main text) examine two distinct but important sources of uncertainty in projections: modeling uncertainty as indicated by the agreement in sign of the projected change for the 13 different models, and internal variability uncertainty, as estimated by statistical significance testing on the 27 different samples (years) from each model's experiments.

SUPPLEMENTAL MATERIAL REFERENCES

Bender MA, Ginis I, Tuleya RE, Thomas B, Marchok T (2007) The operational GFDL coupled hurricane-ocean prediction system and a summary of its performance. Mon Wea Rev 135: 3965-3989

Bender MA, Knutson TR, Tuleya RE, Sirutis JJ, Vecchi GA, Garner ST, Held IM (2010) Modeled impact of anthropogenic warming on the frequency of intense Atlantic hurricanes. Science 327:5964. DOI:10.1126/science.1180568

Dwyer JG, Camargo SJ, Sobel AH, Biasutti M, Emanuel KA, Vecchi GA, Zhao M, Tippett MK (2015) Projected twenty-first-century changes in the length of the tropical cyclone season. J Clim 28:6181–6192. https://doi.org/10.1175/JCLI-D-14-00686.1.

Kalnay E et al (1996) The NCEP/NCAR 40-year re-analysis project. Bull Am Meteorol Soc 77:437–471.

Knutson TR, Sirutis JJ, Garner ST, Held IM, Tuleya RE (2007) Simulation of the recent multidecadal increase of Atlantic hurricane activity using an 18-km-grid regional model. Bull Am Meteorol Soc 88(10). DOI:10.1175/BAMS-88-10-1549.

Knutson TR, Sirutis JJ, Vecchi G, Garner ST, Zhao M, Kim HS, Bender MA, Tuleya RE, Held IM, Villarini G (2013) Dynamical downscaling projections of 21st century Atlantic hurricane activity: CMIP3 and CMIP5 model-based scenario. J Clim 26(17). DOI:10.1175/JCLI-D-12-00539.1.

Tuleya RE, Bender M, Knutson TR, Sirutis JJ, Thomas B, Ginis I (2016) Impact of upper-tropospheric temperature anomalies and vertical wind shear on tropical cyclone evolution using an idealized version of the operational GFDL hurricane model. J Atm Sci 73(10):3803-3820.

Yablonsky RM, Ginis I, Thomas B, Tallapragada V, Sheinin D, Bernardet L (2015) Description and analysis of the ocean component of NOAA's operational Hurricane Weather Research and Forecasting Model (HWRF). J Atm Oceanic Tech, 32(1), 144-163.

Table 1. Summary projections for various Atlantic (basin-wide) or U.S. landfalling TC metrics. Underlined bold text indicates values that are statistically significant at the 0.05 level based on a Mann-Whitney test. Column A (Control) refers to the control run values of the TC metrics, derived from downscaling NCEP Reanalyses (1981-2006). Remaining columns (B-N) refer to percent changes in the TC metric for the given climate change scenario or model, as identified in the "Key to columns" below. The final column ("Average") shows the average of the percent changes in columns B-N, with the value in parentheses indicating the number of models that simulated the same sign change as the average change. "lf" = landfalling storms over the contiguous U.S.; TS = frequency (annual number of storms) of tropical storm-strength (sub-hurricane strength); H1…H5 = frequency of category 1…5 hurricanes; all TCs = frequency of all tropical storms and hurricanes combined; hur (cat 1-5) = frequency of all hurricanes (category 1-5); mhur (cat 3-5) = frequency of major hurricanes of category 3-5; hur45 = frequency of category 4 & 5 hurricanes; lf_TS = frequency of U.S. landfalling sub-hurricane strength storms; lf_all_TCs = frequency of all U.S. landfalling tropical storms and hurricanes; lf_maxwnd_all_TCs = average maximum wind intensity at landfall of U.S. landfalling tropical storms and hurricanes (m s^{-1}); PDI = power dissipation index in units of 10^9 m^3 s^{-2}; max_wind_all_TCs = average lifetime maximum surface wind speed for all tropical storms and hurricanes combined (m s^{-1}); duration = storm accumulated lifetime with at least tropical storm strength (days); trans speed = average propagation speed of storm (m s^{-1}); rain_all_TCs = spatially averaged rain rate within 100 km of storm center for all tropical storm and hurricane, averaged over all time periods where wind intensities exceeded 17.5 m s^{-1} (in mm day^{-1}); lf_rain_all_TCs = average rain rate within 100 km of storm center of all tropical storms and hurricanes at time of U.S. landfall (mm day^{-1}). For basin-wide statistics, results labeled TS, all TCs, or related metrics include track segments where the storm was below tropical storm intensity. Also included were the complete tracks of a small percentage of weak TCs that reached tropical storm status in the parent regional model experiments but never reached tropical storm strength in the downscaled runs. For U.S. landfall proportions, the control values and percent changes are for the fraction of storms of a given category or range of categories that make U.S. landfall. The U.S. landfall proportion is calculated as the ratio of all U.S. landfalling storms to the sum of all landfalling and non-landfalling storms, with storm counts accumulated over all seasons prior to computing the ratio. Statistical significance tests, typically done in the Table by comparing across individual seasons for a given model, were not performed for the U.S. landfall proportions. The PDI for each season is sum of the modeled TC intensities raised to the third power, accumulated over each storm's lifetime and accumulated over the all storms for a season. It is one measure of the aggregate intensity, frequency, and duration combined for TC winds, aggregated over the basin and the entire season.

Key to columns in table.

A	Control	H	CMIP3_mri
B	CMIP3_ens18	I	CMIP3_gfdl-cm20
C	CMIP5_EARLY	J	CMIP3_hadgem1
D	CMIP5_LATE	K	CMIP3_miroc-hi
E	CMIP3_gfdl_cm2	L	CMIP3_ccsm3
F	CMIP3_mpi	M	CMIP3_ingv
G	CMIP3_hadcm3	N	CMIP3_miroc-med

Table 1. Summary Results.

METRIC:	A. Control	Model B	(% C	Change) D	E	F	G	H	I	J	K	L	M	N	Average
Basin-wide frequency															
TS	2.704	-9.6	-2.7	2.7	-9.6	-8.2	-8.2	-16.5	0.0	**-30.1**	4.1	-13.7	-12.4	-28.8	-10.2 (10)
H1	2.37	**-45.3**	-26.5	**-45.3**	-35.9	**-39.1**	**-59.4**	-28.1	-32.8	**-54.7**	**-56.2**	-32.8	-34.3	**-51.6**	-41.7 (13)
H2	1.852	**-56.0**	-10.0	-36.0	**-48.0**	**-52.0**	**-68.0**	**-58.0**	-10.0	**-62.0**	**-60.0**	-18.0	**-50.0**	**-62.0**	-45.4 (13)
H3	2.296	-25.8	**-37.1**	**-33.8**	-24.2	**-58.1**	**-75.8**	-22.6	-17.7	**-79.1**	**-62.9**	-27.4	**-38.7**	**-61.3**	-43.4 (13)
H4	1.37	10.9	-8.1	2.7	24.4	-27.0	**-62.1**	0.0	64.9	**-81.1**	-18.9	0.0	-2.7	-24.3	-9.3 (7)
H5	0.185	80.0	-40.0	120.0	**280.5**	80.0	20.0	120.0	**360.5**	-80.0	20.0	20.0	180.5	80.0	95.5 (11)
all_TCs	10.778	**-24.7**	-17.9	-20.3	-15.8	**-34.0**	**-50.5**	**-23.0**	1.7	**-58.8**	**-37.1**	-19.2	**-24.7**	**-44.0**	-28.3 (12)
hur (cat 1-5)	8.074	**-29.8**	-22.9	**-28.0**	-17.9	**-42.7**	**-64.7**	**-25.2**	2.3	**-68.3**	**-50.9**	-21.1	**-28.9**	**-49.1**	-34.4 (12)
mhur (cat 3-5)	3.852	-7.7	-26.9	-13.5	7.7	**-40.4**	**-66.4**	-7.7	29.8	**-79.8**	**-43.3**	-15.4	-15.4	**-41.4**	-24.6 (11)
hur45	1.556	19.0	-12.0	16.6	54.7	-14.3	**-52.4**	14.3	**99.9**	**-81.0**	-14.3	2.4	19.0	-12.0	3.1 (7)
Landfalling frequency															
lf_TS	0.815	-22.7	-9.1	40.9	4.5	13.6	36.3	0.0	22.7	4.5	-22.7	9.1	54.5	-18.2	8.7 (8)
lf_H1	0.444	-16.7	25.2	16.9	-8.3	-33.3	-66.7	25.2	41.9	-41.7	-8.3	91.9	0.0	-33.3	-0.6 (7)
lf_H2	0.259	-28.6	114.7	28.6	14.3	-57.1	-42.9	0.0	28.6	-42.9	-14.3	14.3	28.6	-42.9	0.0 (--)
lf_H3	0.259	-57.1	42.9	-57.1	28.6	-14.3	-71.4	-42.9	85.7	-71.4	-28.6	-14.3	42.9	-42.9	-15.4 (9)
lf_H4	0.037	300.0	100.0	800.0	**700.0**	0.0	200.0	500.0	**1200.0**	0.0	0.0	0.0	300.0	100.0	323 (9)
lf_all_TCs	1.815	-20.4	26.5	34.7	28.5	-10.2	-10.2	12.2	**63.3**	-24.5	-18.4	26.5	42.9	-26.6	9.6 (7)
lf_hur (cat 1-5)	1	-18.5	55.6	29.6	48.1	-29.6	**-48.1**	22.2	**96.3**	-48.1	-14.8	40.7	33.3	-33.3	10.3 (7)
lf_mhur (cat 3-5)	0.296	-12.5	50.0	50.0	**162.8**	0.0	-25.0	37.5	**237.8**	-62.5	-25.0	-12.5	87.8	-25.0	35.7 (6)
lf_hur45	0.037	300.0	100.0	**800.0**	**1100.0**	100.0	300.0	600.0	**1302.7**	0.0	0.0	0.0	400.0	100.0	392 (10)
Landfalling Intensity															
lf_maxwnd_all_TCs	36.364	-4.0	0.6	-3.3	4.8	-11.3	**-13.0**	-3.4	10.6	**-15.4**	-9.0	-5.3	-1.2	-3.9	-4.1 (10)
lf_maxwnd_hur	45.944	-0.6	-3.7	5.8	**13.6**	3.2	3.5	3.0	11.1	-2.6	-2.5	-5.5	5.3	-0.8	2.3 (7)
Misc. Basin-Wide TC Metrics															
PDI	381.994	-14.0	**-29.0**	-19.1	1.3	**-36.0**	**-65.5**	-20.7	22.1	**-80.5**	**-43.1**	-12.5	-20.0	**-43.4**	-27.7 (11)
max_wind_all_TCs	**43.367**	3.5	-1.4	0.7	7.3	-2.8	**-10.8**	3.6	8.9	**-12.7**	-5.1	1.2	3.3	2.2	-0.2 (5)
max_wind_hur	**49.417**	**8.1**	1.2	**6.0**	**9.7**	4.1	1.4	**5.7**	**10.4**	**-6.9**	6.0	3.4	**6.2**	6.4	4.7 (12)
duration	7.367	-7.1	**-12.1**	-9.1	**-9.9**	**-16.1**	**-28.7**	**-8.9**	-8.8	**-28.1**	**-25.0**	1.3	-8.7	**-12.2**	-13.3 (12)
trans_speed	5.658	3.1	-1.7	2.9	**12.8**	2.8	-2.1	0.5	**10.1**	3.8	3.6	3.7	1.5	-2.5	3.0 (10)
Basin-wide TC Rain-Rate:															
rain_all_TCs	163.2	**24.7**	10.9	**19.5**	**32.8**	21.3	13.8	**21.1**	**29.0**	-9.2	27.5	**14.4**	**18.9**	18.1	18.7 (12)
rain_hur (cat 1-5)	234.252	**23.9**	**10.6**	**23.3**	**29.4**	**24.2**	28.7	**25.8**	**28.7**	1.7	**29.1**	**10.2**	**20.7**	**25.8**	21.7 (13)
rain_mhur (cat 3-5)	341.269	**19.9**	**12.9**	**20.9**	**24.0**	**14.2**	20.3	**21.2**	**25.3**	12.1	21.6	**14.8**	**15.4**	**22.1**	18.8 (13)
rain_hur45	421.257	**24.8**	15.7	**21.9**	**24.3**	7.4	20.0	**22.1**	**20.9**	14.9	25.5	16.5	**17.6**	24.6	19.7 (13)

Table 1, contd.

METRIC:	Model: Control	(%t B	Change) C	D	**E**	F	G	H	**I**	J	K	L	M	N	Average
Landfalling TC Rain Rate:															
lf_rain_all_TCs	169.65	14.5	13.6	24.9	**40.4**	34.3	-4.3	31.5	**43.5**	-11.4	8.1	8.5	19.6	16.2	18.4 (11)
lf_rain_hur (1-5)	223.406	13.9	7.2	**29.3**	**55.2**	44.6	25.4	29.1	**41.7**	8.0	21.4	8.2	31.5	20.0	25.8 (13)
lf_rain_mhur (cat 3-5)	279.786	45.3	6.2	46.8	**51.7**	52.5	36.4	35.7	**38.9**	28.7	24.6	13.5	42.6	55.3	36.8 (13)
lf_rain_hur45	160.66	204.1	52.8	**165.4**	**213.5**	229.2	238.8	**183.4**	**191.9**	157.1	279.5	152.9	**254.0**	186.6	193 (13)
US Landfall proportions															
TS	0.301	-14.5	-6.5	37.1	15.7	23.8	48.6	19.7	22.7	49.6	-25.7	26.4	76.2	14.9	22.2 (10)
H1	0.187	52.4	70.5	113.8	43.0	9.4	-18.0	74.2	111.1	28.7	109.5	185.5	52.3	37.6	66.9 (12)
H2	0.140	62.3	138.5	100.9	119.8	-10.7	78.5	138.0	42.8	50.3	114.2	39.3	157.1	50.3	83.2 (12)
H3	0.113	-42.3	127.1	-35.2	69.6	104.4	18.0	-26.2	125.7	36.4	92.5	18.1	133.1	47.6	51.4 (10)
H4	0.027	260.8	117.6	776.3	543.2	37.0	691.9	500.0	688.4	429.0	23.3	0.0	311.1	164.2	349 (12)
all_TCs	0.168	5.7	54.0	68.9	52.7	36.1	81.5	45.8	60.5	83.1	29.8	56.6	89.8	31.1	53.5 (13)
hur (cat 1-5)	0.124	16.1	101.9	79.9	80.4	22.8	46.9	63.4	91.9	63.9	73.6	78.3	87.5	31.0	64.4 (13)
mhur (cat 3-5)	0.077	-5.2	105.3	73.4	144.1	67.8	122.9	48.9	160.3	85.7	32.2	3.4	122.0	27.9	76.0 (12)
hur45	0.024	236.1	127.2	671.6	675.7	133.5	739.9	512.6	601.6	425.7	16.7	-2.3	320.1	127.2	353 (12)